Summer 2016

Synthetic Investigation on the Biomimetic Metal-Catalyzed Sulfoxidations and Photochemical Generation of a Highly Reactive Ruthenium(V)-Oxo Porphyrin

WeiLong Luo
Western Kentucky University, wielong.luo255@topper.wku.edu

SYNTHETIC INVESTIGATION ON THE BIOMIMETIC METAL-CATALYZED SULFOXIDATIONS AND PHOTOCHEMICAL GENERATION OF A HIGHLY REACTIVE RUTHENIUM(V)-OXO PORPHYRIN

A Thesis
Presented to
The Faculty of the Department of Chemistry
Western Kentucky University
Bowling Green Kentucky

In Partial Fulfillment
of the Requirement for the Degree
Master of Science

Wei Long Luo

August 2016

SYNTHETIC INVESTIGATION ON THE BIOMIMETIC METAL-CATALZED SULFOXIDATIONS AND PHOTOCHEMICAL GENERATION OF A HIGHLY REACTIVE RUTHENIUM(V)-OXO PORPHYRIN

Date Recommended 07-13-16

Dr. Rui Zhang, Director of Thesis

Dr. Eric Conte

Dr. Kevin Williams

7/28/16

Dean, Graduate Studies and Research Date

ACKNOWLEDGMENTS

It is such an honor to express my appreciation to all the amazing people who have contributed to this thesis. This thesis shows not only my work at the keyboard but also a milestone of my remarkable journey in more than three years of work in an organic laboratory at Western Kentucky University. I owe my gratitude to all those people who have helped to make this thesis possible.

My most sincere gratitude goes to my research advisor, Dr. Rui Zhang for his guidance, patience, motivation, understanding and kindness in all respects of my study in WKU. His devoted attitude in research helped me overcome many troubles. I am especially grateful to him for reading and commenting thoroughly on my many revisions of this manuscript. He has always been invaluable on both my academic and personal life.

Besides, I would like to thank the following professors for the valuable suggestions and members of my research group for the wonderful collaboration during the course of my study and compilation of the thesis. It is of great honor to have Dr. Kevin William and Dr. Eric Conte to serve on my thesis committee. Their insightful comments and questions from my research work helped me learn and understand more. In addition, I would thank Ms. Alicia Pesterfield for providing a well-organized chemical stockroom and for her efforts in making the lab a safer environment for the students. I would also like to thank Ms. Haley Smith for general assistance on documents and applications. Moreover, it has been an honor and great privilege working with all former

and present members of my research group: Aaron Carver, Charles Winchester, Davis Ranburger, Haleh Jeddi, Jonathan Malone, Ka Wai Kwong, Ngo Fung Lee, Tse-Hong Chen, and Wesley Bratcher.

I greatly acknowledge the Nation Science Foundation (CHE1213971), (CHE 1464886), Kentucky EPSCoR (REG 2015) and an internal grant from WKU Office of Research (Fuse 13-SP178) for support of this work. Lastly, I have been amazingly fortunate to receive a prestigious scholarship, the Graduate Student Research Fellowship (GSRF), from the Graduate School at WKU which supported me financially throughout my entire graduate study. Most importantly, my family has provided a constant source of love, care, concern, support and courage all over these years. None of these accomplishments would have been possible without my family's support.

ABBREVIATIONS AND SYMBOLS

CYP450s	Cytochrome P450 enzymes
DDQ	2,3-Dichloro-5,6-dicyano-*p*-benzequinone
DMF	*N*,*N*-Dimethylformamide
FID	Flame ionization detector
GC	Gas chromatograph
^{1}H-NMR	Proton nuclear magnetic resonance
H_2TMP	*meso*-Tetramesitylporphyrin
H_2TPP	*meso*-Tetraphenylporphyrin
H_2TPFPP	*meso*-Tetrakis(5,10,15,20-pentafluorophenyl)porphyrin
H_3TPFC	5,10,15-Tri(pentafluorophenyl)corrole
k_0	Background rate constant
k_{obs}	Observed pseudo-first-order rate constant
k_{ox}	Second-order rate constant
LFP	Laser flash photolysis
m-CPBA	*meta*-Chloroperoxybenzoic acid
Mn^{III}(TMP)Cl	5,10,15,20-Tetramesitylporphyrinatomanganese(III) chloride
Mn^{III}(TPP)Cl	5,10,15,20-Phenylporphyrinatomanganese(III) chloride
Mn^{III}(TPFPP)Cl	5,10,15,20-Pentafluorophenylporphyrinatomanganese(III) chloride
$Mn^{III}(TPFC)(OEt)_2$	Manganese(III) 5,10,15-tri(pentafluorophenyl)corrole

MS	Mass spectroscopy
PhIO	Iodosylbenzene
$PhI(OAc)_2$	Iodobenzene diacetate
$Ru^{II}(TPP)(CO)$	Ruthenium(II) carbonyl (5,10,15,20-phenylporphyrinato)
$[Ru^{IV}(TPP)(OH)]_2O$	*bis*-Porphyrin-ruthenium(IV) μ-oxo dimers
TBHP	*tert*-Butyl hydroperoxide
UV-vis	Ultraviolet-visible

TABLE OF CONTENTS

LIST OF FIGURES

Page

LIST OF SCHEMES

Page

LIST OF TABLES

Page

SYNTHETIC INVESTIGATION ON THE BIOMIMETIC METAL-CATALYZED SULFOXIDATIONS AND PHOTOCHEMICAL GENERATION OF A HIGHLY REACTIVE RUTHENIUM(V)-OXO PORPHYRIN

Wei Long Luo August 2016 Pages 65

Directed By: Dr. Rui Zhang, Dr. Eric Conte, Dr. Kevin Williams

Department of Chemistry Western Kentucky University

Catalytic oxidation plays a crucial role in current chemical and pharmaceutical industries which is also a leading technology for green chemical processes. In Nature, the ubiquitous cytochrome P450 enzymes can catalyze a wide variety of oxidation reactions with high efficiency and selectivity. Many transition metal catalysts are designed as the biomimetic model of cytochrome P450 enzymes. In this work, series of metalloporphyrins and metallocorroles have been successfully synthesized to investigate and develop catalytic selective oxidation of sulfides to sulfoxides.

Manganese(III) porphyrin complexes (**2**) and manganese(III) corrole complexes (**6**) with iodobenzene diacetate [$PhI(OAc)_2$] as a mild oxygen source exhibited remarkable catalytic activity toward selective oxidation of sulfides to sulfoxides under mild conditions. Conspicuous is the fact that readily soluble $PhI(OAc)_2$ in the presence of a small amount of water is more efficient than the commonly used PhIO and other oxygen sources under identical conditions. It was found that the reactivity of manganese(III) porphyrin catalysts was greatly affected by axial ligand and the weakly binding chlorate gave the highest catalytic activity in the oxidation of sulfide. Both

porphyrin-manganese and corrole-manganese catalysts catalyzed the highly selective oxidation of *para*-substituted thioanisoles with $PhI(OAc)_2$ in the presence of a small amount of water. Complete conversion and of sulfide and excellent selectivities for sulfoxide were achieved within 120 min.

We discovered that photo-disproportionation of a *bis*-porphyrin-diruthenium(IV)-μ-oxo dimer gave a porphyrin-ruthenium(III) species and a putative poprhyrin-ruthenium(V)-oxo species that can be detected and studied in real time using laser flash photolysis methods. As determined by its spectral and kinetic behavior, the same oxo transient was also formed by photolysis of a porphyrin-ruthenium(III) *N*-oxide adduct. Second-order rate constants for reactions with several substrates at 22 °C were determined; representative values of rate constants were $k_{ox} = 6.6 \times 10^3\ M^{-1}\ s^{-1}$ for diphenylmethanol, $k_{ox} = 2.5 \times 10^3\ M^{-1}\ s^{-1}$ for styrene, and $k_{ox} = 1.8 \times 10^3\ M^{-1}\ s^{-1}$ for cyclohexene.

1. INTRODUCTION

1.1 Catalytic oxidation mediated by cytochrome P450 enzymes

Catalytic oxidation acts as a leading technology in the transformation of petroleum-based materials to high value chemicals such as alcohols, carbonyl compounds or epoxides.[1] The worldwide synthetic application of many useful chemicals ranging from pharmaceutical to large-scale commodities are produced by oxidation reactions.[2] However, conventional oxidation methodologies have still met with limited success due to the low chemo- and/or regio-selectivity as well as low conversion and low turnover number. Some of those are unfavorable in both economical and environmental aspects. Not only the catalyst is costly, an abundance of hazardous waste was also generated.[3] Foremost in oxidation chemistry is the development of new processes that employ transition metals as substrate-selective catalysts and stoichiometric environmentally friendly oxidants such as molecular oxygen or hydrogen peroxide.[4-5] Catalytic oxidation mediated by oxidative enzymes are important in many biosynthesis and biodegradation mechanisms within living systems.[6] Heme-containing oxygenases are involved in many of these biological oxidations. The most common example of these oxygenases is the cytochrome P450 monooxygenase. Largely, this research has been motivated by a family of heme-containing enzymes, namely Cytochrome P450 enzymes (CYP450s). This

family of enzymes is considered categorically as monooxygenases that play a number of crucial biological roles.

CYP450 enzymes are ubiquitous heme-thiolate enzymes which can transfer one oxygen atom from molecular oxygen to a given substrate and subsequently reduce the second oxygen to water, utilizing NADH (nicotinamide adenine dinucleotide) or NADPH (nicotinamide adenine dinucleotide phosphate) as electron donors via electron transport systems (**Scheme 1**).[7] CYP450s are present in a broad range of highly chemo-, regio-, and enantioselective oxidation reactions such as alkene epoxidation and alkane hydroxylation.[6-8] These heme-thiolate enzymes possess a core structure of iron(III) protoporphyrin IX which covalently linked to the protein by the sulfur atom of a proximal cysteine ligand (**Figure 1**).[7] The function of the unique axial cysteine thiolate ligand to the heme iron is thought to control the oxidative reactivity of CYP450s.[9] However, it has been a challenge to modulate the property of CYP450s as electron donor without alternating the conservative heme environment of this enzyme.[10] For instance, mutating the proximal cysteine to histidine which is a residue often found in the corresponding position of non-P450-type heme proteins results in inactivation of CYP450s.[11] Attempts to better understand CYP450s has initiated many research efforts on mechanistic investigations in past decades.

$$\text{R-H} + O_2 + \text{NADPH} + H^+ \xrightarrow{\text{CYP450}} \text{R-OH} + H_2O + \text{NADP}^+$$

Scheme 1. Monooxygenase reaction.

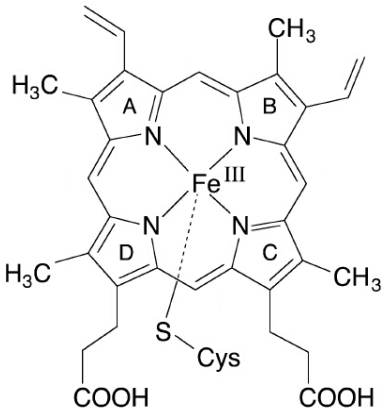

Figure 1. Iron(III) protoporphyrin IX linked with a proximal cysteine ligand.

The name of CYP450s comes from the reduced form of the enzyme which efficiently binds carbon monoxide that gives a strong absorption at 450 nm.[12] CYP450s are typically membrane-bound to the endoplasmic reticulum of microsomal membranes and the inner mitochondrial membrane.[7] New CYP450s are continuously being discovered. Thus far, there are approximately 8,100 distinct CYP450s genomes that have been identified. CYP450s are ubiquitously found in human beings, bacteria, insects, fungi and many other living systems. They may be isolated from intestine, kidney, lung, and liver tissues.[13] One of the most characterized CYP450s is the camphor P450 monooxygenase found within *Pseudomonas putida* by Gunsalous and co-workers (**Figure 2**).[7] The three-dimensional structure of $P450_{cam}$ was provided by Poulos et al. in 1986. $CYP450_{cam}$ catalyzes the stereospecific hydroxylation of the *exo* C-H bond at position 5 of camphor (**Scheme 2**).[12] Significant efforts have been made toward the creation of artificial versions of this impressive enzyme.

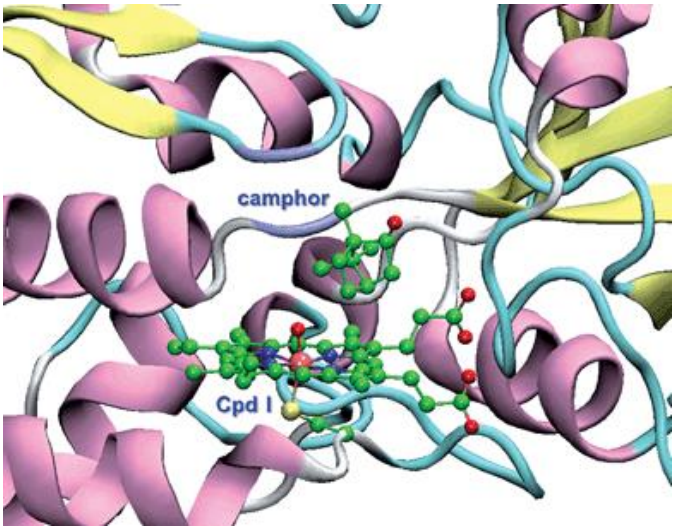

Figure 2. X-ray structure of cytochrome $P450_{cam}$.

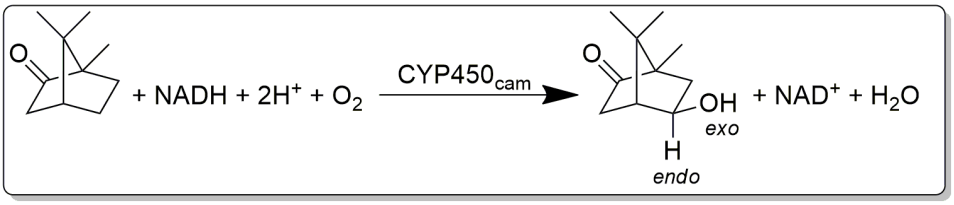

Scheme 2. Stereospecific hydroxylation of the *exo* C-H bond at position 5 of camphor by cytochrome $P450_{cam}$.

Even fifty years after the discovery of CYP450s, the true oxidizing species is still elusive.[12] The highly reactive oxidant CYP450s is thought to be an iron(IV)-oxo porphyrin radical cation termed as Compound I, which is by analogy to the intermediates formed in peroxidase and catalase enzymes.[14] In this regard, many synthetic metalloporphyrin complexes have been implemented as model catalysts in a variety of selective oxidation reactions. (**Scheme 3**).[12] Largely, this work has been devoted to mechanistic investigations on biomimetic CYP450s models.

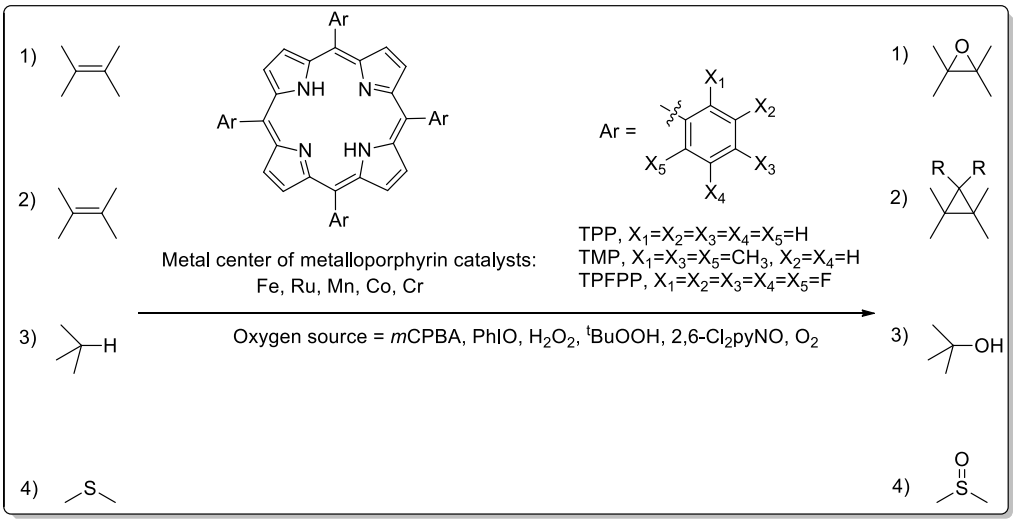

Scheme 3. Typical metalloporphyrin-catalyzed oxidation reactions.

1.2 Biomimetic models of metalloporphyrins

Metalloporphyrins containing manganese, ruthenium or iron are typically used as biomimetic models of cytochrome P450 enzymes in a variety of oxidation reactions which may act as viable catalysts. The first biomimetic oxidation catalyzed by an iron porphyrin was reported by Groves and co-workers in 1979, which implemented an iron porphyrin catalyst with an oxygen source of iodosylbenzene to mediate effective stereospecific alkene epoxidation and alkane hydroxylation (**Scheme 4**).[15] Effective oxidation systems utilizing metalloporphyrins with numerous oxygen sources such as iodosylbenzene, sodium hypochlorite and 2,6-dichloropyridine *N*-oxide, have extensively been investigated and reported.[16-17]

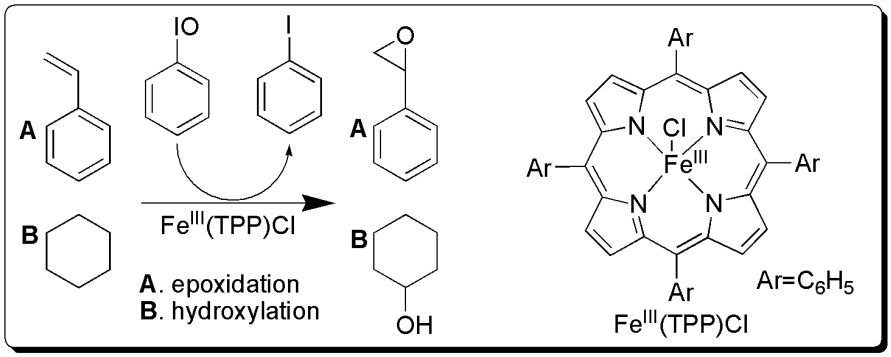

Scheme 4. Alkene epoxidation and alkane hydroxylation catalyzed by Fe^{III}(TPP)Cl.

Generally, oxidation of transition metal catalysts by sacrificial oxidants results in the formation of high-valent metal-oxo compounds. These high-valent metal-oxo species have the ability to oxidize various organic substrates. A high-valent iron-oxo species was characterized by the oxidation of Fe^{III}(TMP)Cl with *m*-CPBA under low temperature.[12] According to the report by Groves et al. in 1997, a highly reactive manganese(V)-oxo porphyrin complexes were isolated and characterized in olefin epoxidation and alkane hydroxylation.[18]

Ruthenium porphyrin species have drawn much attention due to the periodic relationship to iron and their abilities to act as biomimetic catalysts for hydrocarbon oxidations. The ruthenium metal ion possesses a wide range of oxidation states from -2 to +8.[19] Ruthenium complexes possess a variety of valuable attributes for oxidation chemistry such as rich coordination, low redox potential, high stability and high electron transfer ability.[6] One distinct example is the carbonyl ruthenium(II) tetrapentafluorophenyl porphyrin efficiently catalyzes the hydroxylation of alkanes, the

cleavage of ethers, and the oxygenation of benzene with 2,6-dichloropyridine *N*-oxide (**Scheme 5**).[19]

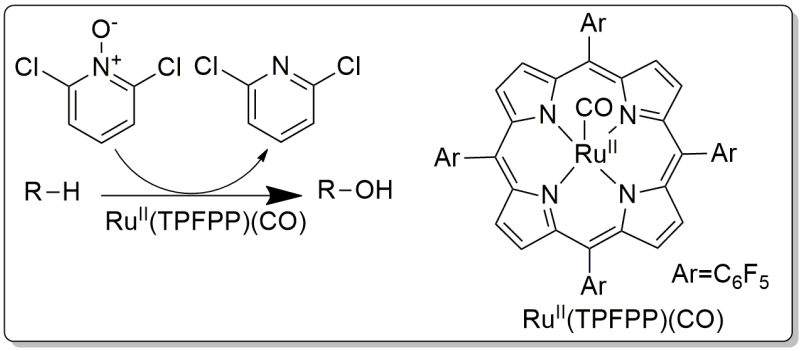

Scheme 5. Hydroxylation of hydrocarbons catalyzed by Ru^{II}(TPFPP)(CO).

1.3 Biomimetic models of metallocorroles

The cobalt-chelating corrin in vitamin B_{12} (**Figure 3**) can be attributed to a tetrapyrrolic macrocycle ligand known as corrole which is structurally similar to a porphyrin compound.[20] Corrole is a tri-anionic ligand characterized by three *meso* carbon positions with a pyrrole-pyrrole linkage, one imino group, and three amino groups (**Figure 4**). The more electron-rich system allows the tri-anionic corrole ligands to support higher metal oxidation states than the porphyrin counterpart.[21] Corrole exhibits asymmetric intensity in the Soret band and a weak Q-band in the UV-vis spectroscopy and is considered to be more acidic to porphyrin.[22] Many studies focused on meso-trairyl-substituted corroles owing to the recent advance of corrole synthesis.[23]

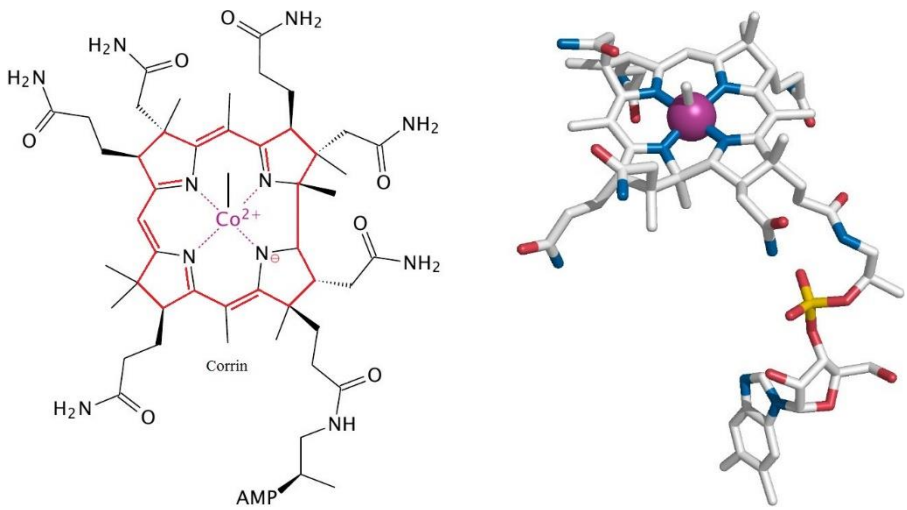

Figure 3. Structure of vitamin B_{12}.

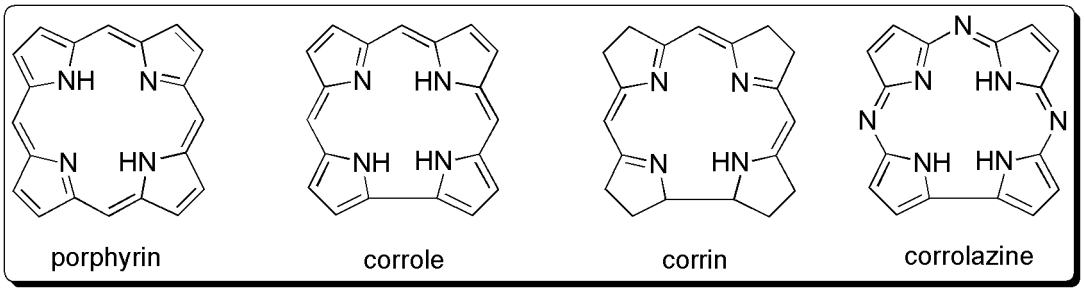

Figure 4. Structures of porphyrin, corrole, corrin and corrolazine.

The first corrole synthesis was reported by Johnson's group in 1965.[24] Until recently, most investigations into corrole focused on its synthesis and the coordination chemistry of metallocorrole complexes. The method of solvent-free condensation of pyrrole and aldehyde discovered by Gross and co-workers in 1999 allows for an efficient synthetic pathway to prepare corroles.[23] Due to the innovative discovery of corrole synthesis, metallocorrole complexes including corrolazines have gained increased attention (**Figure 4**).

Catalytic oxidation using PhIO with iron(IV) complex of tris(pentafluoro)corrole was first reported in 1999 by Gross and co-workers.[25] The same authors also studied

biomimetic oxidations with manganese (III) corrole , albumin-conjugated manganese and chromium corroles.[26-27] Meanwhile, manganese and iron corrolazines as oxidation catalysts have also been investigated by Goldberg and co-workers.[28] Metallocorroles exhibit a reduced stability compared to metalloporphyrins and are therefore susceptible to oxidative degradation. For this reason, the choice of oxygen source is critical in regard to the stability and reactivity in the metallocorrole mediated oxidations.

1.4 Sulfoxidation reactions

The selective oxidation of sulfide to sulfoxide is of great importance in synthetic chemistry.[29] Catalytic selective sulfoxidations are commonly used in the synthesis of a variety of chemically and biologically significant molecules. In addition, these reactions are important from green chemistry and industrial perspectives because organosulfur reagents are major pollutants.[30] Sulfoxides are valuable in medicinal and pharmaceutical chemistry to generate various therapeutic agents such as antiulcer, antifungal, antibacterial, cardiotonic, anti-atherosclerotic and antihypertensive drugs.[31] To develop highly selective sulfoxidation reactions, a variety of electrophilic reagents like peracids, hypochlorite, sodium periodate, iodosobenzene, peroxyacids and highly toxic metal oxidants have been employed for the oxidation of conventional sulfides.[32]

Since Marcker reported the sulfoxidation in 1865, many different reagents and methods have been developed for transformation of sulfide to the corresponding sulfoxide. Although many different reagents may be used in sulfoxidation reactions, most of them are not satisfactory, in view of their costliness, toxicity, or selectivity for sulfoxide formation.[29,33] According to the application of sulfoxidation reactions by

Kowalski and co-workers, utilizing hydrogen peroxide as a green oxidant carried out a direct conversion of sulfide to sulfoxide without generating toxic by-products.[29] However, many reported methods have still met with limited success due to long reaction times and over oxidation to sulfone.

Given that clean and safe oxidants such as hydrogen peroxide or molecular oxygen are viable, studies on catalytic epoxidations, hydroxylations and sulfoxidations by transition metal complexes with sacrificial oxygen sources have gained considerable attention is the search for new, green applications.[34] Investigation of iodobenzene diacetate as a mild oxygen source has scarcely been studied in relation to catalytic sulfoxidations by manganese porphyrin and corrole complexes. In this work, we aim to explore the potential of manganese porphyrin and corrole complexes toward catalytic sulfoxidation reactions with iodobenzene diacetate as the oxygen source under mild catalytic conditions.

1.5 High-valent metal-oxo oxidizing intermediates

High-valent transition metal-oxo transients are thought to be the active oxidizing species in synthetic and natural oxidation catalysts.[12] In some cases, metal-oxo species can be observed through spectroscopic methods such as rapid mixing technique, or by production of lower-reactivity analogues.[35] However, the reactive metal-oxo species typically does not accumulate to detectable quantities, and the actual oxidizing species remains speculative.

Studies of transition metal oxidation catalysts remain complicated due to the lack of kinetic and mechanistic information. In many cases, the nature of the active oxidants was

inferred from product studies. Successful generation and characterization of the reactive metal-oxo species may provide insights into chemical models of the enzyme-like oxidants and should ultimately aid in catalyst design for selective oxidation of various organic substrates within industrial process.[36]

In this work, we attempt to produce high-valent ruthenium-oxo species by photo-disproportionation and photo-induced ligand cleavage reactions. Through kinetic studies we attempt to characterize the reactivity of the ruthenium(V)-oxo transient toward various organic substrates.

2. EXPERIMENTAL SECTION

2.1 Materials

All organic solvents were purchased from Aldrich Chemical Co. for synthesis and purification. A comprehensive solvent list is as follows: acetone, acetonitrile, benzene, chloroform, decalin, dichloromethane, ethanol, ethyl acetate, methanol, hexane and *N*,*N*-dimethylformamide (DMF). All substrates including thioanisole, 4-methoxy thioanisole, methyl *p*-tolyl sulfide, 4-fluorothioanisole, 4-chlorothioanisole, and 4-bromothioanisole were obtained from Aldrich Chemical Co., and further purified by a dry column chomatograph on alumina gel (neutral). The pyrrole was freshly distilled before use. Iodobenzene diacetate [$PhI(OAc)_2$], hydrogen peroxide,iodosylbenzene (PhIO), *tert*-butyl hydroperoxide (TBHB), *meta*-choloroperoxybenzoic acid (*m*-CPBA), mesitaldehyde, boron trifluoride diethyl etherate ($BF_3 \cdot Et_2O$), 2,3-dichloro-5,6-dicyano-*p*-benequinone (DDQ), decahydronaphthalene (decalin), triruthenium dodecacarbonyl, tetra(pentafluorophenyl) porphyrin (H_2TPFPP), 2,3,4,5,6-pentafluorobenzaldehyde, manganese (II) acetate tetrahydrate, and triruthenium dodecacarbonyl were used as received. The stock solutions of manganese (III) porphyrin complexes with different axial ligands was readily prepared by stirring with the corresponding silver salts, leading to the formation of $Mn^{III}(Por)(ClO_4)$, $Mn^{III}(Por)$ (ClO_3), $Mn^{III}(Por)(NO_3)$ and $Mn^{III}(Por)(NO_2)$.

2.2 Physical measurements

UV-vis spectra were recorded on an Agilent 8453 diode array spectrophotometer (Figure 5A). Gas chomatograph analyses were performed on Agilent GC7820A-MS5975 equipped with a flame ionization detector (FID) and coupled with an auto sample injector (Figure 5B). Collection of the ^{1}H-NMR spectra was conducted on a JEOL CA-500 MHz FT-NMR spectrometer at 298 K with tetramethylsilane (TMS) as internal standard.

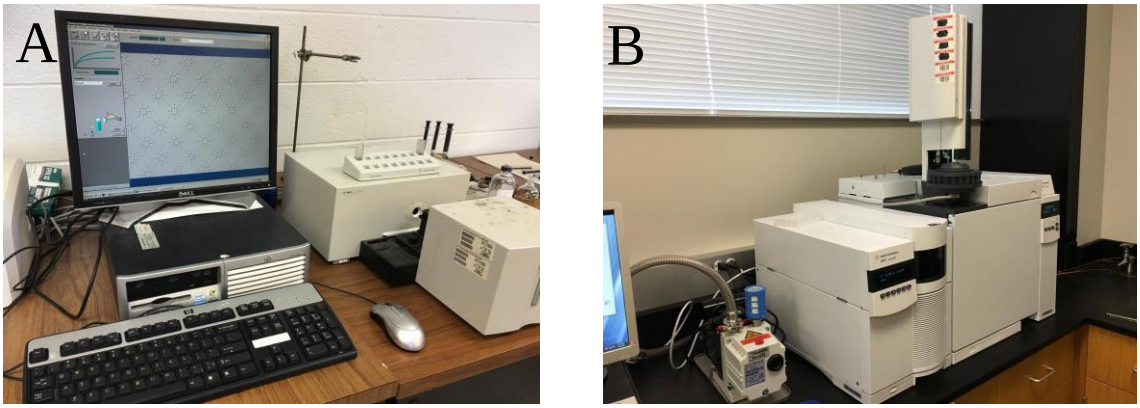

Figure 5. (A**)** Agilent 8453 diode array UV-visible spectrophotometer. (B) Agilent GC-MS system.

2.3 General procedure for catalytic sulfoxidations

The typical catalytic sulfoxidation reaction procedure was composed of manganese porphyrin or manganese corrole catalysts (1 μmol) in a solution (0.5 mL) consisting of a small amount of H_2O, organic substrate (0.2 mmol) and $PhI(OAc)_2$ (0.3 mmol) as oxygen source. The solution was stirred at 23 ^{o}C ± 2 ^{o}C. Aliquots of the reaction solutions were analyzed by ^{1}H-NMR or GC analysis with J&W Scientific cyclodex-B capillary column to determine the substrate conversions and product yields.

2.4 Synthesis and spectroscopic characterization

2.4.1 *meso*-Tetramesitylporphyrin [H_2TMP] (**1a**)

As shown in **Scheme 6**, the porphyrin free ligand (**1a**) was synthesized according to the literature method described by Lindsey's group.[37] Freshly distilled pyrrole (347 μL, 5 mmol) and mesitaldehyde (736 μL, 5 mmol) were first dissolved in the solvent (500 mL) chloroform in a round bottom flask with a fitted reflux condenser. Ethanol (3.2 mL), serving as a co-catalyst, was then added to the solution. Argon gas was used to purge the solution for about 5 min. Boron trifluoride diethyl etherate (660 μL, 1.65 mmol) was added into the solution in a dropwise manner. The solution was stirred for approximately 3 h under room temperature. The reaction was monitored by UV-vis spectroscopy and TLC analyses. Following condensation of pyrrole and mesitaldehyde, DDQ (957 mg) was added to the flask and the solution was gently refluxed for 1 h. After the solution cooled to room temperature, excess triethylamine (230 μL, 1.65 mmol) was added to the solution to neutralize the remaining acid. The resulting solid crude product was washed using an excess amount of methanol under vacuum filtration until the filtrate was colorless. The product was further purified by wet column chomatography on silica gel with dichloromethane as eluent. A purple powdery product of *meso*-tetramesitylporphyrin (**1a**) (179 mg) was obtained after removing the solvent and characterized by UV-vis (Figure 6) and ^{1}H-NMR (**Figure 7**).

[H_2TMP] (**1a**) Yield = 18.3%. ^{1}H-NMR (500 MHz, $CDCl_3$): δ, ppm: -2.50 (s, 2H, NH), 1.81 (s, 24H, ortho-CH_3), 2.62 (s, 12H, *p*-CH_3), 7.26 (s, 8H, *m*-ArH), 8.61 (s, 8H, *β*-pyrrole).

[H_2TMP] (**1a**) UV-vis (CH_2Cl_2) λ_{max}/nm: 418 (Soret), 513, 593

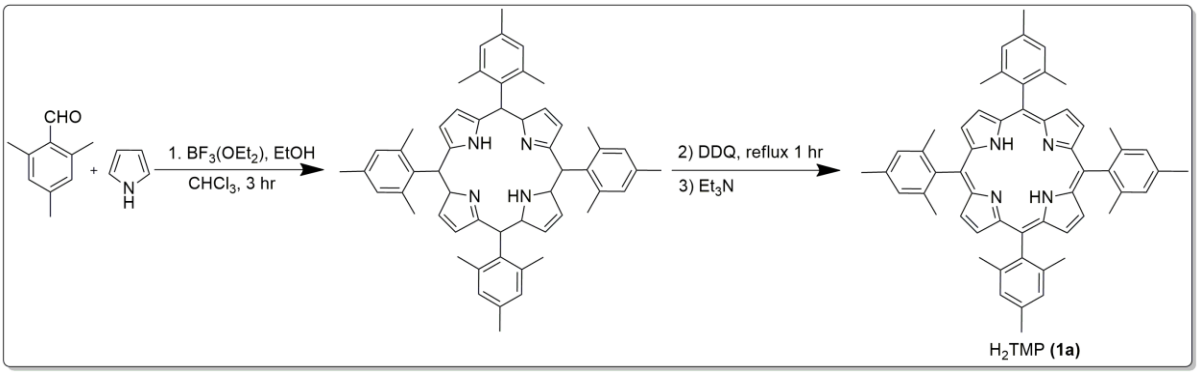

Scheme 6. Two-step synthesis of H_2TMP (**1a**).

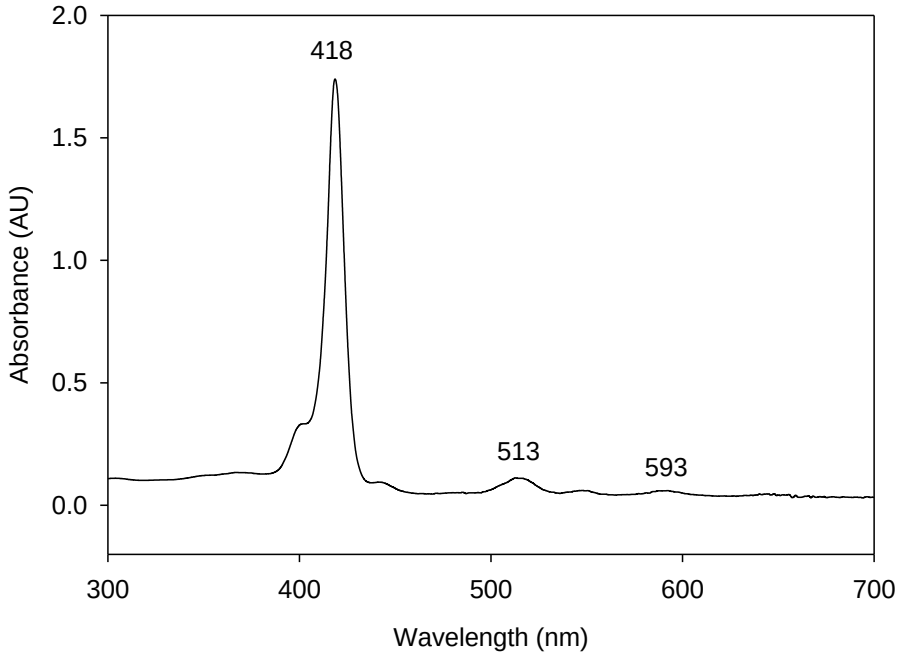

Figure 6. The UV-vis spectrum of H_2TMP (**1a**) in CH_2Cl_2.

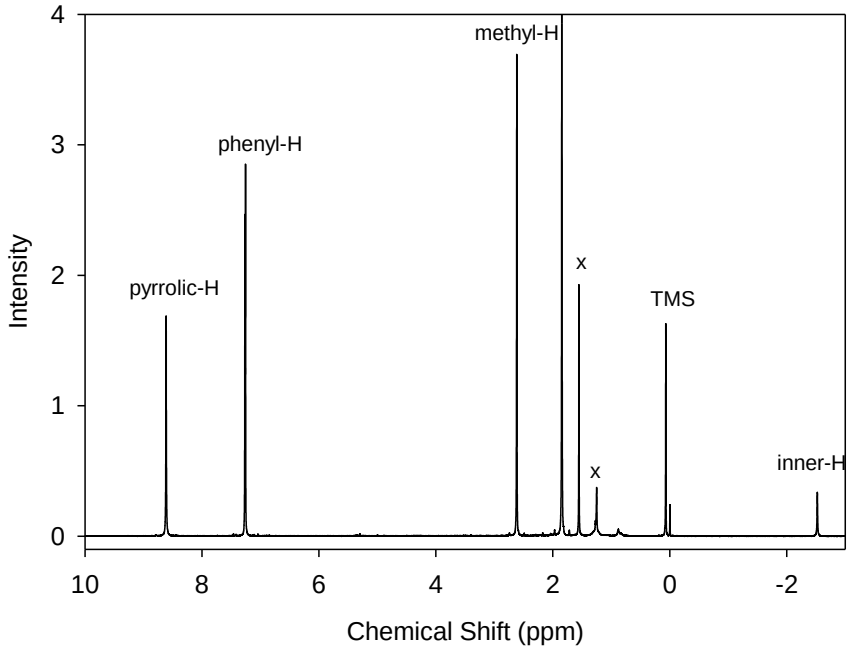

Figure 7. The ^{1}H-NMR spectrum of H_2TMP (**1a**) in $CDCl_3$.

2.4.2 *meso*-Tetraphenylporphyrin [H_2TPP] (**1b**)

According to the literature method described by Adler as shown in **Scheme 7**,[38] freshly distilled pyrrole (5 mL, 7.2 mmol) and benzaldehyde (7 mL, 7.2 mmol) were added to propionic acid (350 mL) in a round-bottom flask and gently refluxed for 30 min under continuous stirring. The mixture was then cooled to room temperature, and followed by vacuum filtration. The crude product was washed with an excess amount of methanol. The resulting product was dried under vacuum and a purple crystalline powder was obtained with an 18.5% yield. The free porphyrin ligand (**1b**) was characterized by UV-vis (**Figure 8**) and ^{1}H-NMR (**Figure 9**)

[H_2TPP] (**1b**) ^{1}H-NMR (500MHz, $CDCl_3$): δ, ppm: 8.85 (pyrrolic H, 8H), 8.21 (s, 16 H), 7.76 (s 4H), -2.81(s, 2H)

[H_2TPP] (**1b**) UV-Vis (CH_2Cl_2) λ_{max}/nm: 415 (Soret), 513, 545, 590, 646.

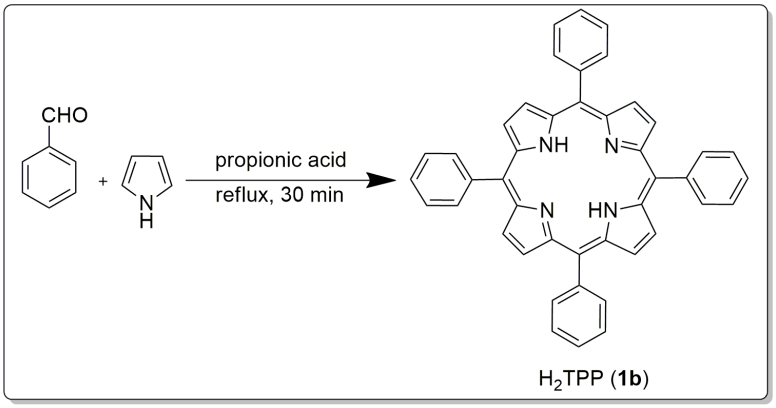

Scheme 7. Synthesis of H_2TPP (**1b**).

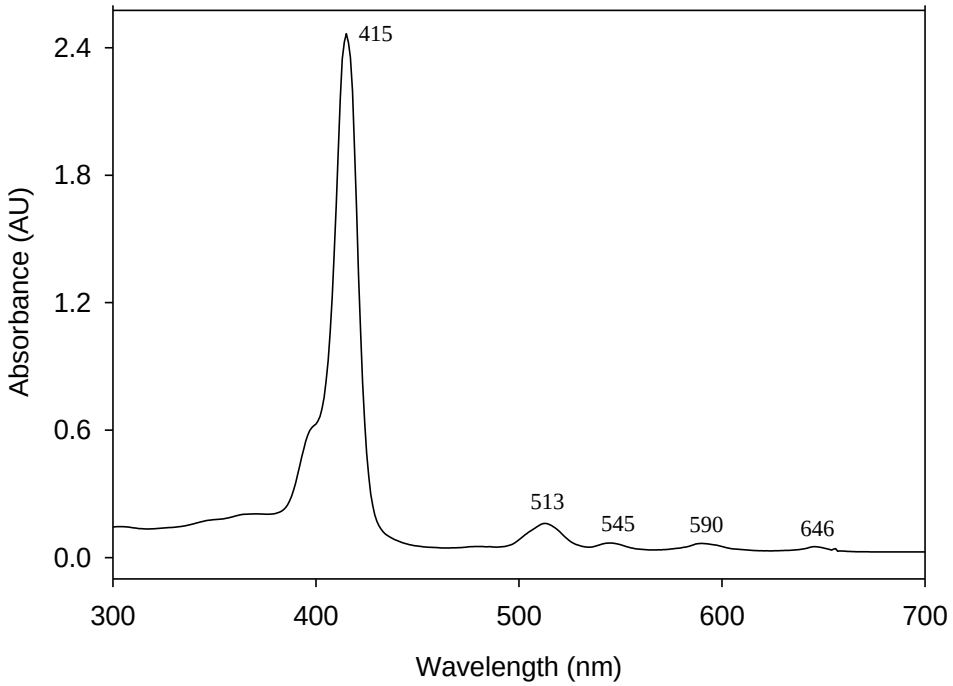

Figure 8. The UV-vis spectrum of H_2TPP (**1b**) in CH_2Cl_2.

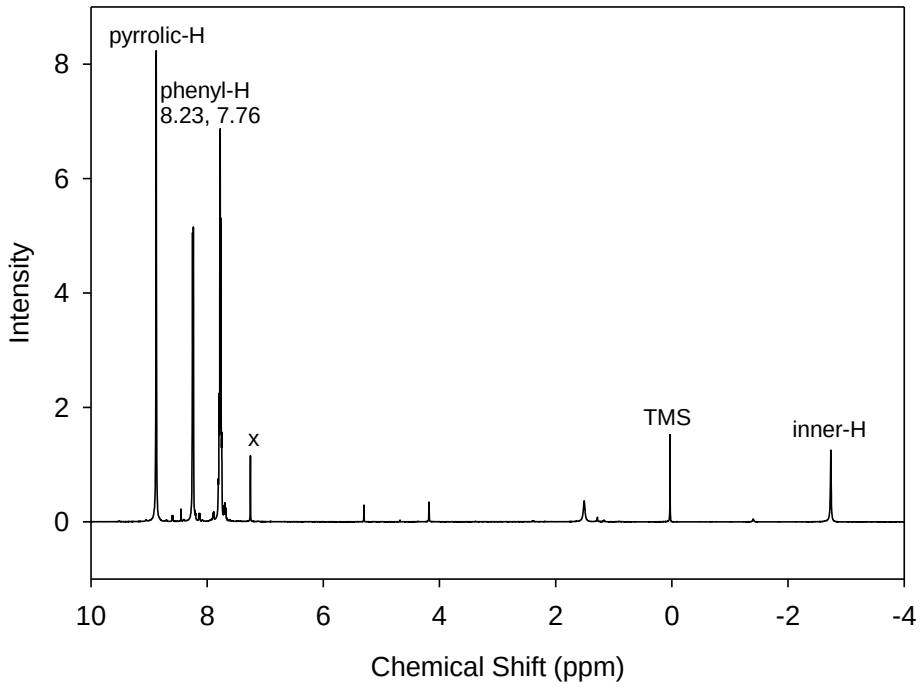

Figure 9. The ^{1}H-NMR spectrum of H_2TPP (**1b**) in $CDCl_3$.

2.4.3 Manganese (III) chloride porphyrin [Mn^{III}(Por)Cl] (**2**)

According to the literature procedure shown in **Scheme 8**,[39] free ligand (**1a**) (100 mg) or a commercially available porphyrin free ligand of 5,10,15,20-tetrakis(pentafluorophenyl) porphyrin (H_2TPFPP) (**1c**) and an excess amount of manganese(III) acetate tetrahydrate (300 mg) were dissolved in DMF (30 mL). The mixture was purged with argon for 5 min and gently heated to reflux with stirring for 30 min. Both complexes were successfully synthesized in the same manner except that the complex (**2a**) requires a longer refluxing time. The Soret band of the metalated porphyrin complex was monitored by UV-vis spectroscopy and TLC analyses. The DMF solvent was removed by vacuum distillation and the crude product was then dissolved in

dichloromethane. The axial ligand was readily replaced by chloride ion when hydrochloric acid (6M) was added to the solution and stirred for 30 min. After removing HCl though extraction, the residual solution was evaporated to dryness and further purified by a wet column chomatograph on silica gel. The metalated porphyrin complexes were characterized by UV-vis as shown in **Figure 10** and **11**, matching the reported values.[39]

[Mn^{III}(TMP)Cl] (**2a**) Yield = 78% (78 mg) UV-vis (CH_2Cl_2) λ_{max}/nm: 480 (Soret), 377, 584, 619

[Mn^{III}(TPPFPP)Cl] (**2c**) Yield = 85% (85 mg) UV-vis (CH_2Cl_2) λ_{max}/nm: 474 (Soret), 364, 573

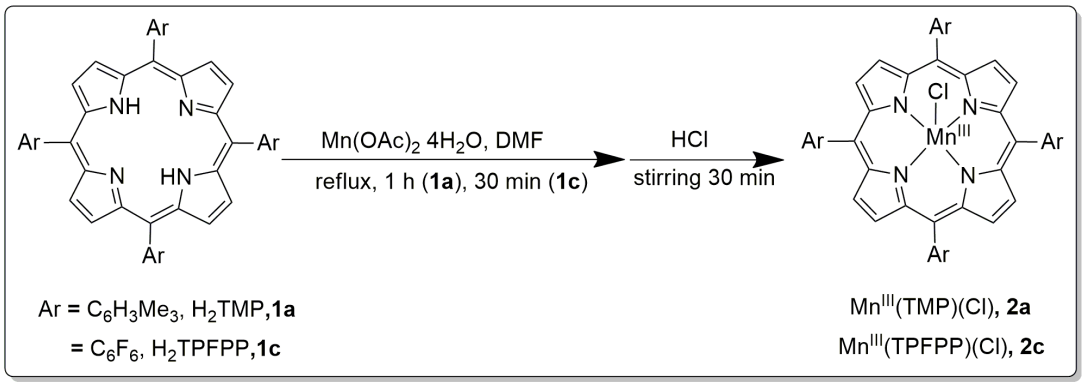

Scheme 8. Synthesis of Mn^{III}(Por)Cl (**2**).

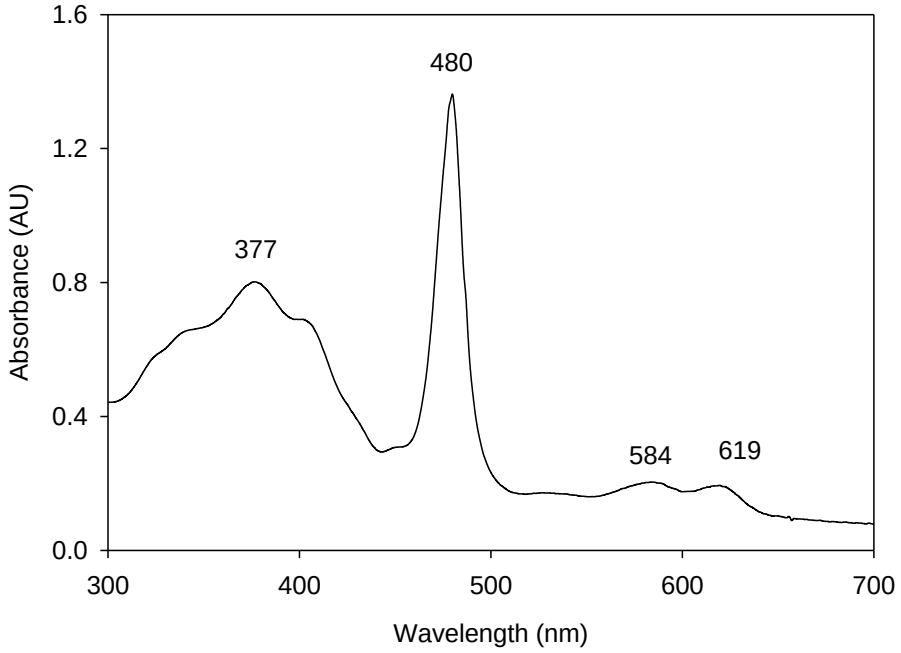

Figure 10. The UV-vis spectrum of Mn^{III}(TMP)Cl (**2a**) in CH_2Cl_2.

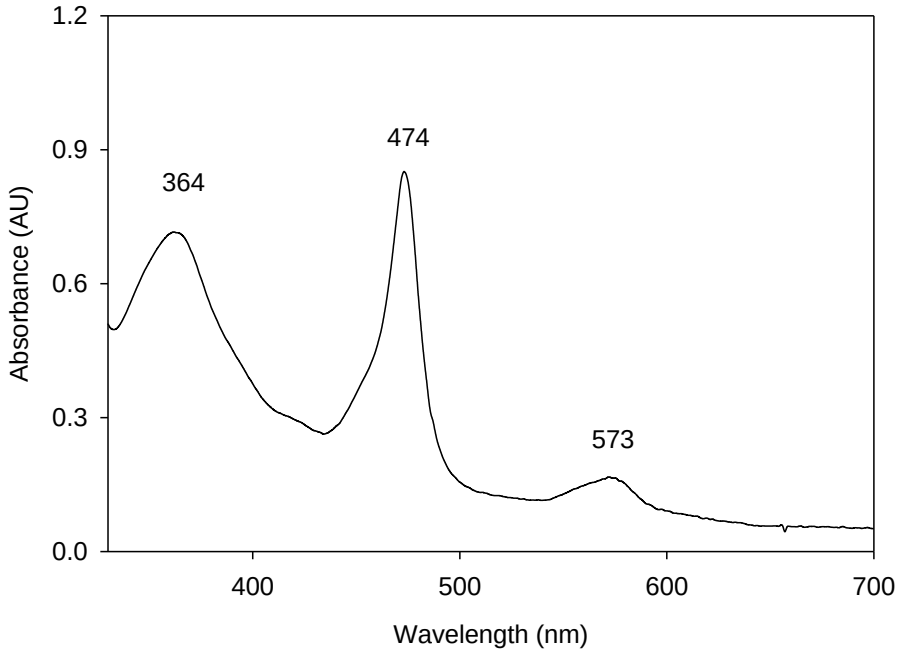

Figure 11. The UV-vis spectrum of Mn^{III}(TPFPP)Cl (**2c**) in CH_2Cl_2.

2.4.4 Axial ligand exchange reactions

The stock solution of $Mn^{III}(TPFPP)(ClO_3)$ (**2d**) was readily prepared by ligand exchange with corresponding silver salts. $Mn^{III}(TPFPP)(Cl)$ (**2c**) (1 mg) was added to a solution of $CHCl_3$ (0.1 mL). An excess amount of $AgClO_3$ (1 mg) was dissolved in a small amount (few drops) of CH_3CN then added into the porphyrin solution. Immediately, a color change was noticed and AgCl precipitate was formed that was then filtered off. The clean filtrate gave the $Mn^{III}(TPFPFF)(ClO_3)$. The entire transformation was monitored by UV-vis spectroscopy (**Figure 12**).

The preparation of $Mn^{III}(TPFPFF)(ClO_4)$, $Mn^{III}(TPFPFF)(NO_3)$, and $Mn^{III}(TPFPFF)(NO_2)$ as shown in **Scheme 9**, are similar to the procedure described for $Mn^{III}(TPFPFF)(ClO_3)$. The products with corresponding axial ligands were characterized by UV-vis (**Figure 13**).

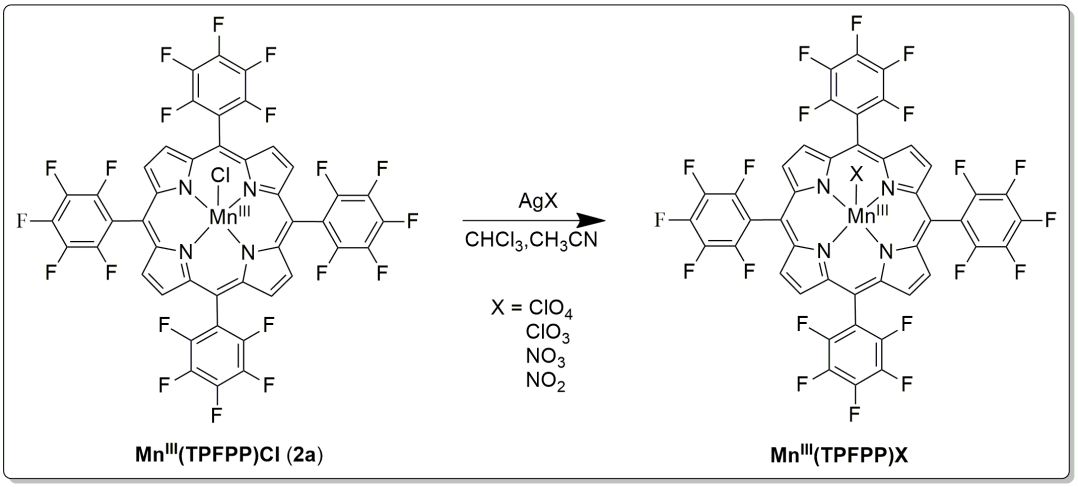

Scheme 9. Synthesis of $Mn^{III}(TPFPP)X$

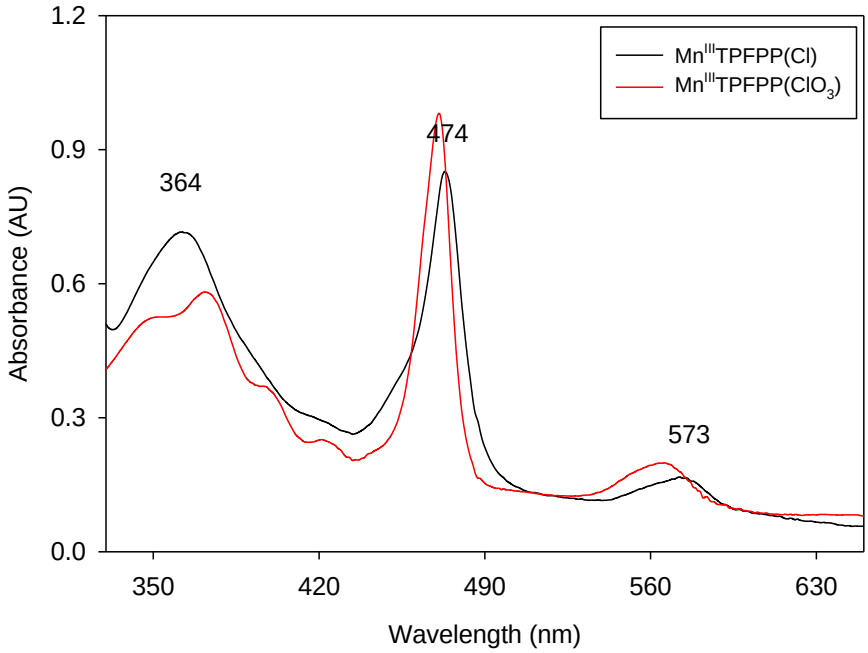

Figure 12. UV-vis spectrum of Mn^{III}(TPFPP)Cl (**2c**) (black line) and Mn^{III}(TPFPP)(ClO_3) (**2d**) (red line)

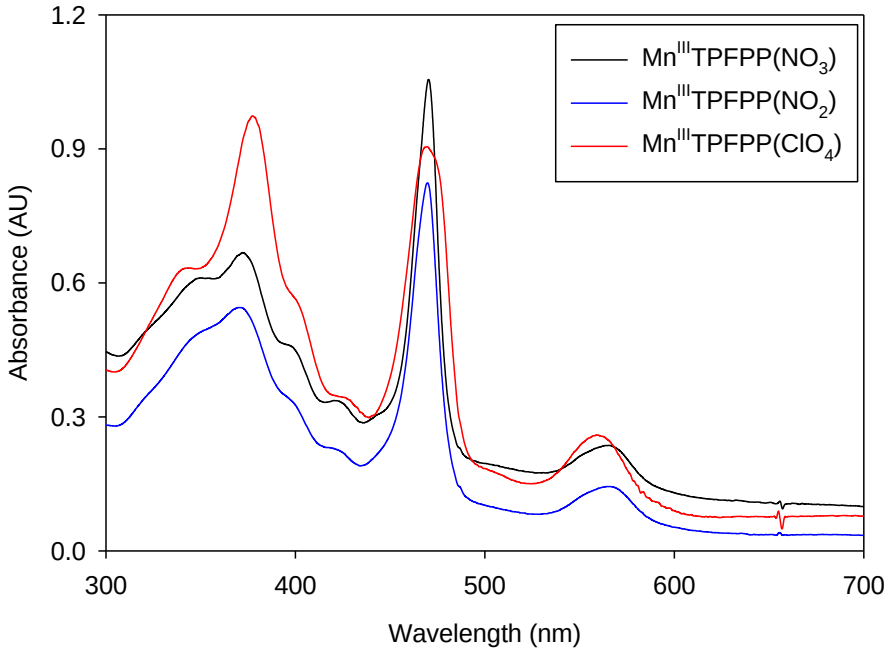

Figure 13. UV-vis spectrum of Mn^{III}(TPFPP)(NO_3) (black line), Mn^{III}(TPFPP)(NO_2) (blue line), and Mn^{III}(TPFPP)(ClO_4) (red line).

2.4.5 Ruthenium(II) carbonyl porphyrin [Ru^{II}(TPP)(CO)] (**3**)

The preparation of ruthenium(II) carbonyl porphyrin complex proceeded according to the reported method described by Che and coworkers (**Scheme 10**).[40] Free porphyrin ligand (H_2TPP) (**1b**) (100 mg) was dissolved in decalin (50 mL) in a round-bottom flask and gently heated with stirring to ca. 100 ^{o}C. An excess amount of triruthenium dodecacarbonyl [$Ru_3(CO)_{12}$] (100 mg) was added and the solution was refluxed at 180 ^{o}C for 1.5 h. UV-vis was used to monitor the process with the Soret band at 411 nm of the metal complex according to the reported values. The mixture was cooled to room temperature and wet column chomatography (Al_2O_3, basic) was used for product purification. A large excess amount of hexane was first used to remove decalin followed by the removal of unreacted free ligand using dichloromethane. The eluent of acetone:dichloromethane (1:1, v/v) was then used to elute the desired product. A brick-red solid of Ru^{II}(TPP)(CO) (**3**) was obtained (100 mg) with a 90% yield after the removal of solvent. The metalloporphyrin (**3**) was characterized by UV-vis (**Figure 14**), matching the literature values.[40]

[Ru^{II}(TPP)(CO)] (**3**) UV-Vis (CH_2Cl_2) λ_{max}/nm: 409 (Soret), 527

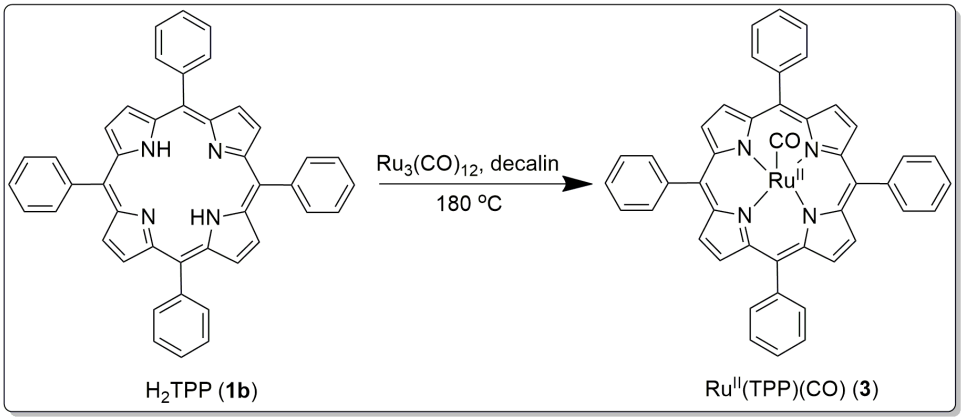

Scheme 10. Synthesis of Ru^{II}(TPP)(CO) (**3**).

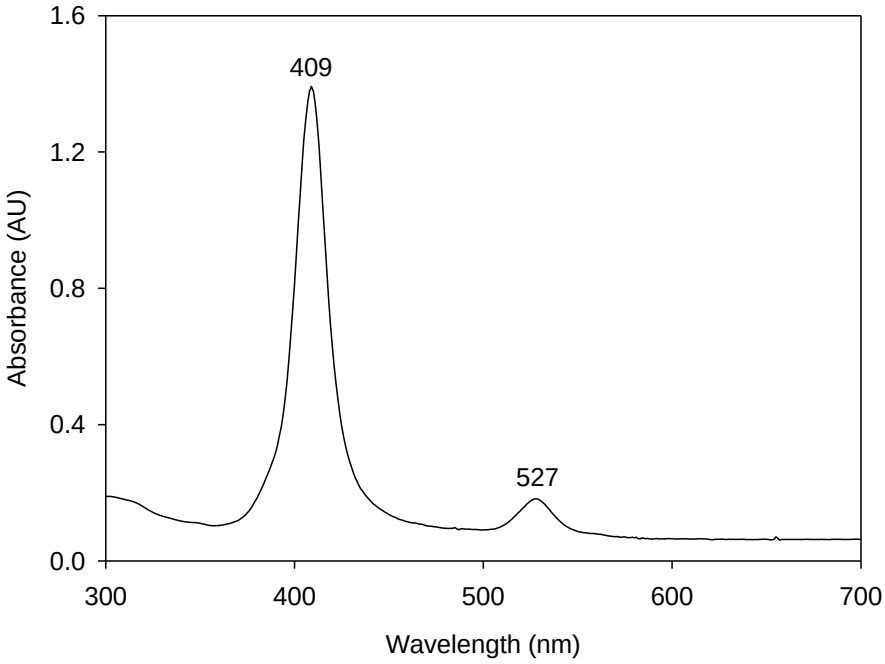

Figure 14. UV-vis spectrum of Ru^{II}(TPP)(CO) (**3**).

2.4.5 *bis*-Porphyrin-ruthenium(IV) μ-oxo dimers $[Ru^{IV}(TPP)(OH)]_2O$ (**4**)

The bisporphyrin-ruthenium(IV) μ-oxo dimer was prepared according to the well-known method decribed by Sugimoto and others,[41] as shown in **Scheme 11**. A mixture of $Ru^{II}(Por)(CO)$ (**3**) (50 mg) in benzene (50 mL) with 70% aqueous *tert*-butyl hydroperoxide (0.5 mL) was stirred at room temperature until the reaction underwent a color change from orange red to dark brown. After the removal of solvent under reduced pressure, wet column chomatography on alumina gel was used to purify the product with dichloromethane as eluent. A purple greed solid (45 mg) with a 90% yield was obtained after removing the solvent via rotary evaporation. The characterization data of desired product $[Ru^{IV}(TPP)(OH)]_2O$ (**4**) was consistent with the reported values.[41]

$[Ru^{IV}(TPP)(OH)]_2O$ (**4**) ^{1}H-NMR (500MHz, $CDCl_3$): δ, ppm: 8.9 (d, H_0), 8.6 (s, pyrrolic H), 7.9, 7.4 (d, $H_{m,\,p}$), -3.9 (axial ligand, OH)

$[Ru^{IV}(TPP)(OH)]_2O$ (**4**) UV-Vis (CH_2Cl_2) λ_{max}/nm: 393 (Soret), 522

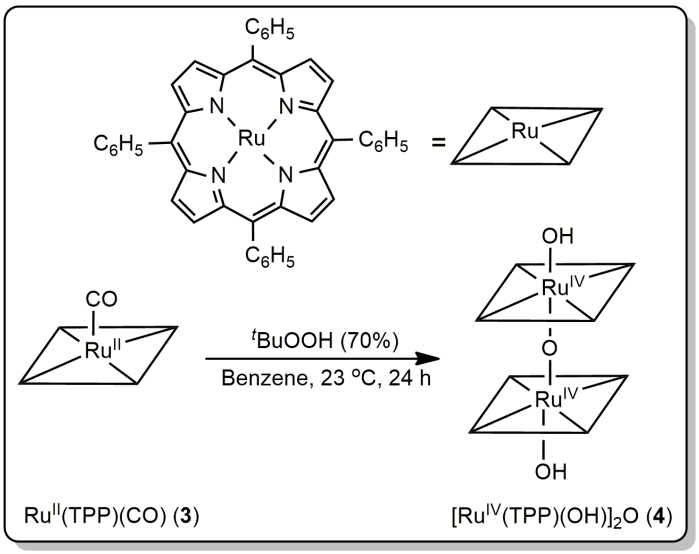

Scheme 11. Synthesis of $[Ru^{IV}(TPP)(OH)]_2O$ (**4**)

2.4.6 5,10,15-Tri(pentafluorophenyl)corrole [H_3TPFC] (**5**)

The corrole free ligand was synthesized according to the solvent-free condensation method described by Gross and coworkers,[23] as shown in **Scheme 12**. Pentafluorobenzadehyde (1.85 mL, 15 mmol) and freshly distilled pyrrole (1.04 mL, 15 mmol) were dissolved in dichloromethane (5 mL). The mixture was transferred to a 50 mL round-bottom flask containing a solid support (Al_2O_3, 3 g) and heated to 60 ^oC with stirring in an open vessel. The reaction was maintained at 60 ^oC for 4 h after the dichloromethane was completely evaporated. A dark reddish-brown tarry product was formed. The tarry product was dissolved in dichloromethane and filtered under vacuum to remove excess Al_2O_3. The filtrate was stirred with DDQ for 1 h. TLC and UV-vis were used to monitor the reaction throughout the process. Further purification was performed by subsequent wet columns (silica gel) with hexane/dichloromethane (5:1, v/v) as the eluent. A dark purple solid product was obtained after the removal of solvent. The structure of H_3TPFC (**3**) was confirmed by UV-vis (**Figure 15**) and ^{1}H-NMR (**Figure 16**), matching the literature values.[23]

[H_3TPFC] (**5**) Yield = 7 %. ^{1}H-NMR (500 MHz, $CDCl_3$): δ, ppm: 2.25 (broad singlet, 3H), 8.57 (d, 4H), 8.75 (d, 2H), 9.10 (d, 2H).

[H_3TPFC] (**5**) UV-vis (CH_2Cl_2) λ_{max}/nm: 407 (Soret), 562, 603.

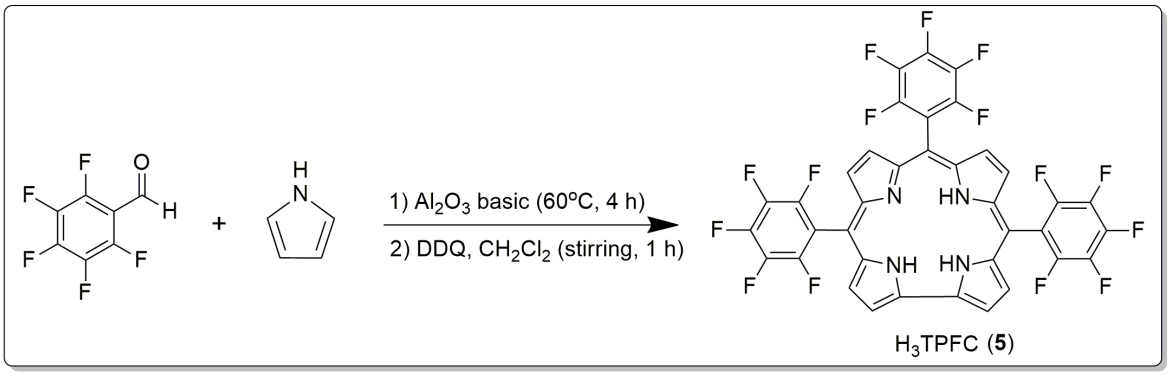

Scheme 12. Synthesis of H_3TPFC (**5**)

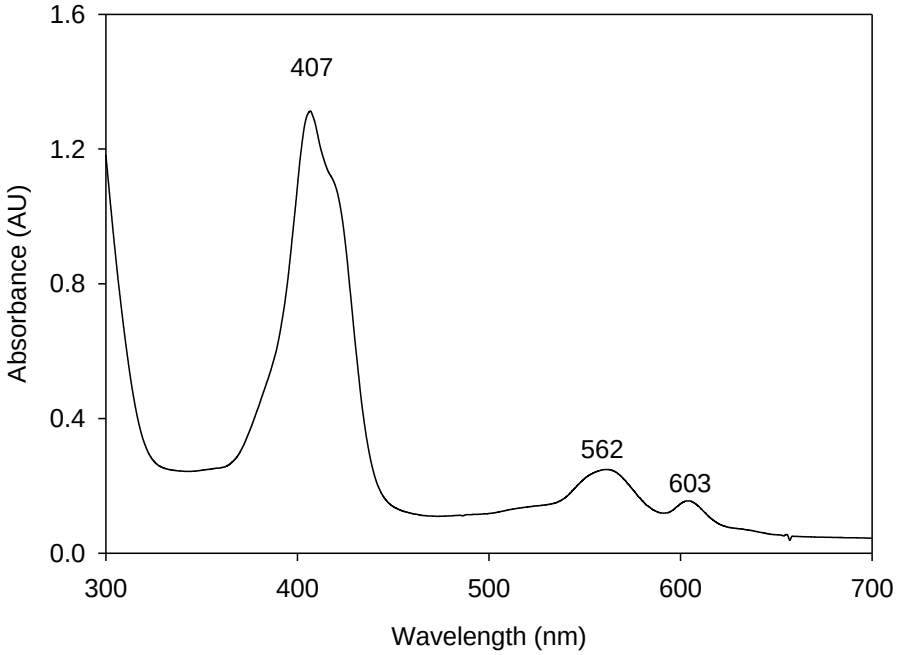

Figure 15. The UV-vis spectrum of H_3TPFC (**5**) in CH_2Cl_2.

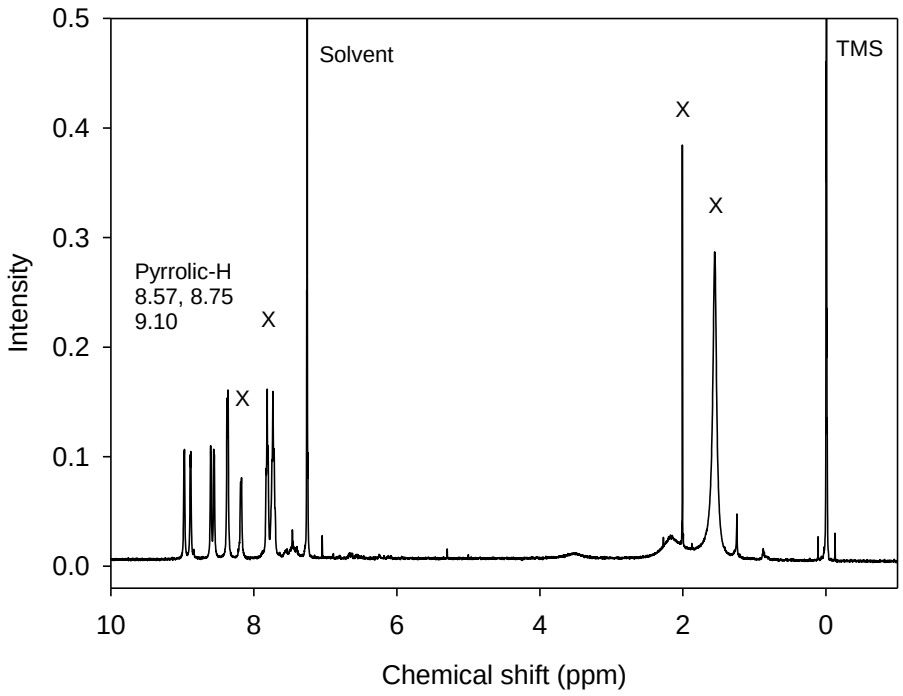

Figure 16. The ^{1}H-NMR spectrum of H_3TPFC (**5**) in $CDCl_3$.

2.4.7 Manganese(III) corroles [Mn^{III}(TPFC)(OEt_2)$_2$] (**6**)

Following the metalation method described by Gross and others,[42] manganese corrole complex was successfully synthesized (**Scheme 13**). H_3TPFC (**5**) (100 mg) was dissolved in DMF (30 mL) in a 50 mL round-bottom flask fitted with a reflux condenser. The mixture was purged with argon for 5 min. Manganese (II) acetate tetrahydrate (300 mg) was added to the solution, which was gentle heated to reflux for 20 min. UV-vis was used to monitor this process. After the evaporation of DMF though vacuum distillation, the crude product was then dissolved in diethyl ether and purified by wet column chomatography on silica gel with diethyl ether as eluent. A shiny, dark green solid (83 mg) was obtained. UV-vis was used to identify the final product (**Figure 17**).

[Mn^{III}(TPFC)·(OEt_2)$_2$] (**6**) Yield = 83% UV-vis (CH_2Cl_2) λ_{max}/nm: 395, 414, 481, 600

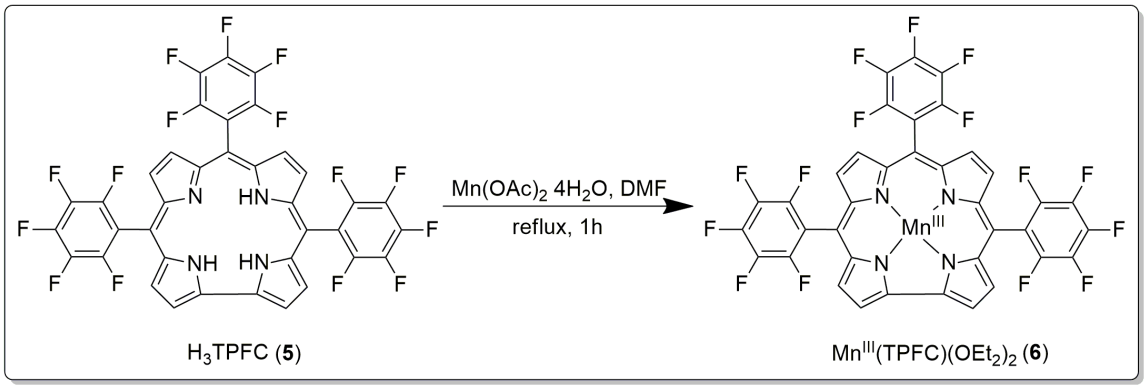

Scheme 13. Synthesis of $Mn^{III}(TPFC)(OEt_2)_2$ (**6**).

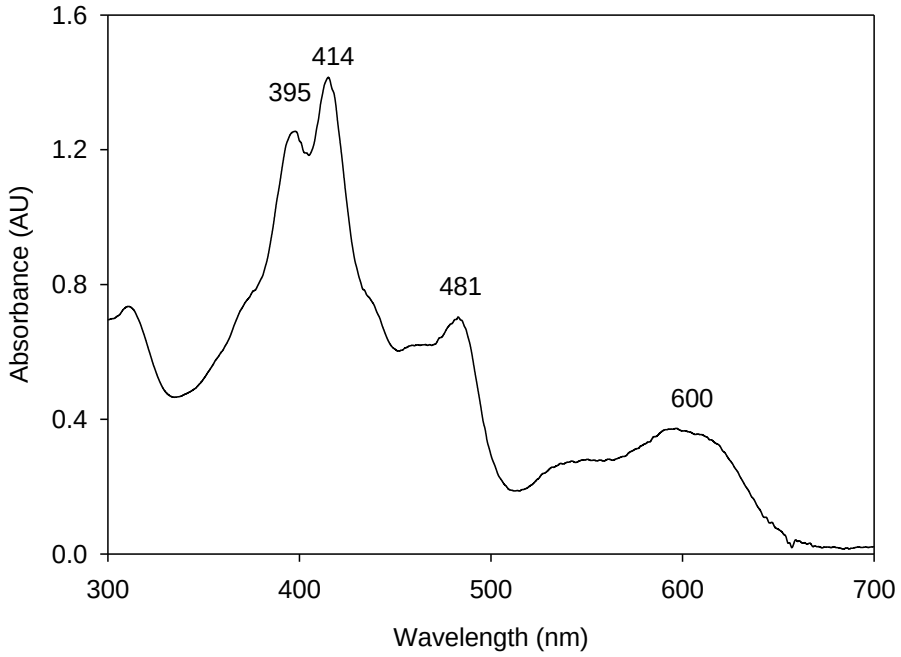

Figure 17. The UV-vis spectrum of $Mn^{III}(TPFC)(OEt_2)_2$ (**6**) in CH_2Cl_2.

3. SELECTIVE SULFOXIDATION CATALYZED BY MANGANESE PORPHYRIN AND MANGANESE CORROLE CATALYSTS

3.1 Introduction

Synthetic manganese(III) porphyrins have been extensively studied as the biomimetic model of P450 enzymes in oxidation reactions.[12,21] In recent decades, there have been a large number of reports on the catalytic behavior of manganese(III) porphyrins with emphasis on alkane oxidation. In general, catalytic applications involve the oxidation of organic substrates through a single oxygen transfer mechanism in the presence of sacrificial oxygen sources such as *meta*-chloroperoxybenzoic acid (*m*-CPBA), PhIO, hydrogen peroxide, and organic peroxide. In our previous work, manganese(III) porphyrin complexes exhibited remarkable catalytic activity towards the selective oxidation of alkenes and activated hydrocarbons with iodobenzene diacetate [$PhI(OAc)_2$] as the oxygen source.[43] However, the oxidation of sulfide catalyzed by manganese(III) porphyrins or corroles with $PhI(OAc)_2$ remains unattempted.

Due to advances in the synthesis of 19-membered macrocyclic triarylcorroles, metallocorrole species have drawn increased attention due to their similar structural and catalytic properties to metalloporphyrins.[44-45] In this work, we aim to investigate both manganese(III) corrole and porphyrin species as promising catalytic candidates in various sulfoxidation reactions using iodobenzene diacetate $PhI(OAc)_2$ as a mild oxygen source.

$PhI(OAc)_2$ is commercially available, readily soluble in organic media and easy to handle. Notably, it does not show appreciable reactivity towards organic substrates nor does it damage the porphyrin/corrole catalyst under the typical catalytic conditions. In this section, we discover efficient oxidation of sulfide with $PhI(OAc)_2$ catalyzed by manganese(III) porphyrin and corrole complexes. In most cases, *para*-substituted thioanisoles have been successfully oxidized to corresponding sulfoxides with quantitative conversion and excellent selectivity.

3.2 Results and discussions

3.2.1 Screening studies

Despite the common use of $PhI(OAc)_2$ as a mild oxygen source for past decades, only few studies have been reported thus far on metalloporphyrin and/or metallocorrole-mediated sulfoxidation reactions by $PhI(OAc)_2$. Therefore, we first investigated the usefulness of $PhI(OAc)_2$ as oxygen source in the catalytic oxidation of thioanisole (**7**) with different manganese (III) porphyrin and corrole complexes (**2a**, **2c**, and **6**) to identify the optimal conditions through screening studies.

Under homogenous conditions, sulfoxidation reactions were carried out with catalyst (0.5 mol%) and a ratio (1:1.5) of thioanisole and $PhI(OAc)_2$ at room temperature and followed by product analysis through ^{1}H-NMR and/or gas chromatography (GC). In previous studies, we found that the addition of a small amount of water to the manganese(III) porphyrin-catalyzed epoxidations with $PhI(OAc)_2$ was crucial to accelerate reactions.[43] The time courses of sulfoxidation reactions by $Mn^{III}(TPFPP)(ClO_3)$

were depicted in the presence and absence of water in **Figure 18**. This plot shows an elevated reaction rate with the addition of water, consistent with previous studies.[43] A similar acceleration of reaction rate due to water was observed in the previously reported iron(III) porphyrin/corrole-catalyzed oxidations.[46] The increased rate was rationalized in terms of the formation of the more oxidizing PhIO. Water is a dissociating solvent and helps remove the axial ligand to efficiently bind the oxygen source. These findings indicate that accessibility of the oxygen source to the metal center might be crucial to reactivity.

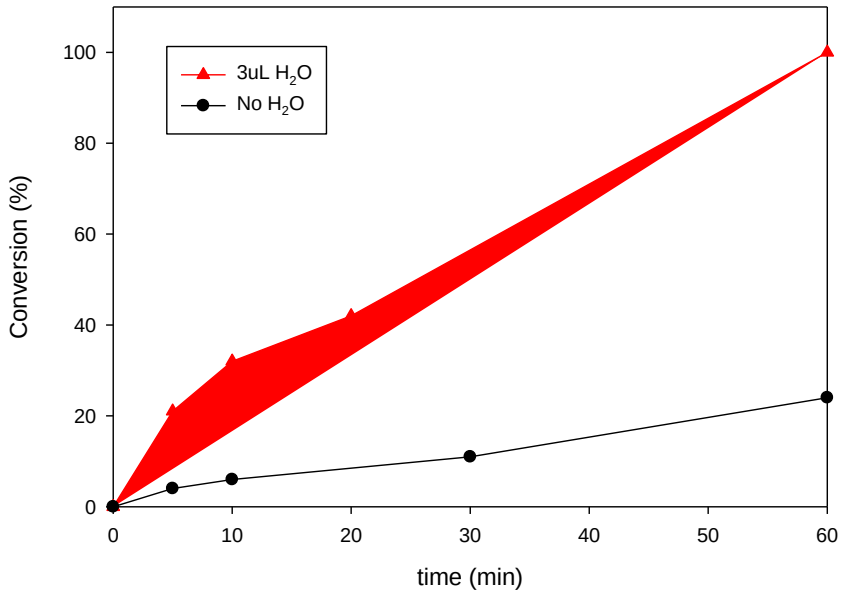

Figure 18. Time course of sulfoxidation of sulfide (**7**) (0.2 mmol) with $PhI(OAc)_2$ (0.3 mmol) in $CHCl_3$ (0.5 mL) catalyzed at room temperature by $Mn^{III}(TPFPP)(ClO_3)$ (**2d**) (0.1 µmol) in the presence (triangle) or absence (circle) of water (3 µL). Aliquots were taken at selected time intervals for product analyses by GC.

According to the results collected in Table 1, the oxidation of **7** catalyzed by $Mn^{III}(TPFPP)Cl$ (**2c**) was relatively slow in the absence of water, and an 11% conversion

of sulfide was obtained over 60 min (entry 1, **Table 1**). Remarkably, the same reaction proceeded more rapidly with the addition of water (5 μL), and 64% conversion was obtained after 60 min (entry 2, **Table 1**). Utilizing a less electron-deficient porphyrin system, i.e. Mn^{III}(TMP)Cl (**2a**) resulted in lower conversions (Table 1, entries 4 and 5).

To further explore the potential of $PhI(OAc)_2$, a corrole catalyst Mn^{III}(TPFC) (**6**) was also employed. With the addition of water, 91% conversion was observed (**Table 1**, entry 7), as compared to 40% conversion in the absence of water (**Table 1**, entry 6). The use of CH_3CN, CH_2Cl_2 or $CHCl_3$ as a solvent instead of CH_3OH resulted in reduced activity, presumably due to the low solubility of $PhI(OAc)_2$ in those solvents (**Table 1**, entries 7, 9 and 10). Surprisingly, a rapid reaction in the solvent of CH_3OH was obtained with 100% conversion of sulfide within 20 min. albeit with a reduced selectivity, 88% of sulfoxide and 12% of sulfone were observed (**Table 1**, entry 8). The cause of a reduced selectivity may result from the enhanced reactivity of the reaction.

Table 1. Catalytic oxidation of thioanisole by manganese porphyrin and corrole with $PhI(OAc)_2$ [a]

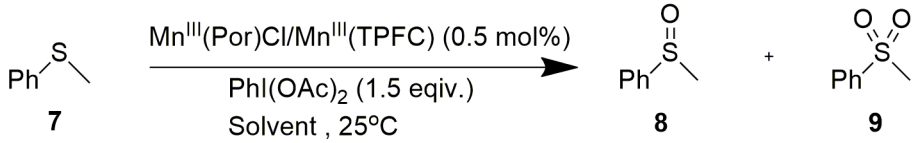

Entry	Catalyst	Solvent	Time (min)	Conversion (%)[b]	Selectivity (7a:7b)[b]
1	Mn^{III}(TPFPP)Cl (**2c**)	$CHCl_3$	60	11	90:10
2[c]			60	64	82:10
3		CH_3CN	60	12	100:0
4	Mn^{III}(TMP)Cl (**2a**)	CH_3CN	60	2.6	100:0
5		$CHCl_3$	60	5	100:0
6	Mn^{III}(TPFC) (**6**)	CH_3CN	60	40	97:3
7[c]			60	91	86:14
8[c]		CH_3OH	20	100	84:16
9[c]		CH_2Cl_2	90	100	88:12
10[c]		$CHCl_3$	90	100	92:8

[a] All reactions were performed under catalyst (1.0 μmol), $PhI(OAc)_2$ (0.3 mmol), thioanisole (0.2 mmol), solvent (0.5 mL), water (5μL), 25 ºC. [b] Conversions and product selectivity were determined by GC-MS analysis with an internal standard (1,2,4-trichlorobenzene) in the crude reaction mixture. [c] Reaction with 5 μL H_2O.

3.2.2 Axial ligand effect

It is well-documented in literature that the axial ligand has a significant effect on the reactivity of high-valent metal-oxo porphyrin intermediates toward organic substrates.[47-48] It has been shown that axial ligands of iron(III) porphyrin complexes play an important role in the catalytic oxidation of hydrocarbons with various terminal

oxidations, in which the yields of oxidized products were markedly dependent on the axial ligands of the iron(III) porphyrin catalyst.[49-50] In this regard, we carried out a series of sulfoxidation reactions catalyzed by Mn^{III}(TPFPP)X with different axial ligands (X = Cl^-, ClO_4^-, ClO_3^-, NO_3^-, and NO_2^-) and investigated their efficacy in the sulfoxidation of thioanisole (**Table 2**). Reactions of the manganese(III) porphyrin chloride with the following silver salts (X): $AgClO_4$, $AgClO_3$, $AgNO_3$, and $AgNO_2$ gave solutions of the corresponding Mn^{III}(TPFPP)(X) salts. Formation of these species were confirmed by the UV-vis spectra, and were consistent with the reported values.[50]

Under identical conditions, the results in Table 2 show that axial ligands of manganese porphyrin catalysts have a marked influence on the formation rate of sulfoxide (**7a**). It was found that Mn^{III}(TPFPP)(ClO_3) was the most efficient catalyst, yielding a complete conversion of thioanisole within 30 min (**Table 2**, entry 5). Lower conversion of sulfide was observed when Mn^{III}(TPFPP)X (X=ClO_4, NO_3, NO_2) were used under identical conditions. The lowest conversion was obtained with Cl^- as the axial ligand, which has the strongest coordinating ability to the metal center in contrast with the axial ligand of ClO_3^- (**Table 2**, entry 1). The comparison of different *meso*-substituted groups on the porphyrin structure shows that a highly electron-deficient porphyrin (TPFPP > TPP > TMP) gave the highest product conversion (**Table 2**, entries 5-7). Hence, the axial ligand effect on the oxidation of sulfide is possibly attributed to rapid reaction of Mn^{III}(TPFPP)(ClO_3) with $PhI(OAc)_2$ to generate the active oxidizing species.

Table 2. Axial ligand effect on the manganese(III) porphyrin-catalyzed sulfoxidation reaction with $PhI(OAc)_2$.[a]

Entry	Catalyst	Axial ligand	Time (min)	Conversion (%)[b]	Selectivity (7a:7b)[b]
1	$Mn^{III}(TPFPP)X$	Cl	60	64	82:18
2		NO_3	60	97	90:10
3		NO_2	60	73	90:10
4		ClO_4	60	81	88:12
5		ClO_3	30	100	96:4
6	$Mn^{III}(TMP)X$	ClO_3	30	69	99:1
7	$Mn^{III}(TPP)X$	ClO_3	30	82	99:1

[a] All reactions were performed with catalyst (1.0 μmol), $PhI(OAc)_2$ (0.3 mmol), thioanisole (0.2 mmol), chloroform (0.5 mL), water (5μL), 25 °C. [b] Conversions and product selectivity were determined by GC-MS analysis with an internal standard (1,2,4-trichlorobenzene) on the crude reaction mixture.

3.2.3 Comparison of various oxygen sources

The promising results with $PhI(OAc)_2$ in **Table 1** prompted us to evaluate other common oxygen sources in the manganese(III) corrole-catalyzed sulfoxidation of thioanisole. A screening of diverse oxygen sources under identical experimental conditions disclosed that the mild oxygen source, $PhI(OAc)_2$, was especially effective and selective for oxidation of sulfide to sulfoxide as representative results show in **Table 3**. Although iodosobenzene (PhIO) is a more common oxygen source used for metalloporphyrin-mediated oxidations, it was found that the use of the more soluble

$PhI(OAc)_2$ for sulfoxide reactions under the same conditions gave sulfoxide selectiviely with a higher substrate conversion (**Table 3**, entry 1 and 3).

Lowering the amount of $PhI(OAc)_2$ in this oxidation resulted in reduced activity (**Table 3**, entry 2). The use of a stronger oxidizing oxygen source (*m*-CPBA) gave complete conversion albeit with undesirable sulfone formation (**Table 3**, entry 4). It is possible that use of stronger oxygen sources may lead to increased reactivity of the manganese(III) corrole catalysts and subsequently result in the over oxidation of sulfoxide to sulfone. The application of hydrogen peroxide (H_2O_2) and *tert*-butyl hydroperoxide (TBHP) resulted in the lowest catalytic activity under the established conditions, giving less than 5% conversion (**Table 3**, entries 5 and 6). The most likely explanation is that the catalyst was bleached during the reaction by these powerful oxygen sources. These results conclude that the choice of oxygen source is critical in regards to catalyst stability and reactivity in these metallocorrole catalyzed oxidations. In comparison to the other oxidants, $PhI(OAc)_2$ not only exhibited high chemoselectivity but also showed enhanced stability of the catalyst in this particular sulfoxidation.

Table 3. Catalytic oxidation of thioanisole by the Mn^{III}(TPFC) (**6**) with various oxygen sources.

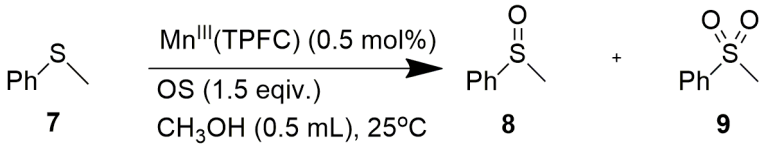

Entry	Oxygen source (OS)	Conversion (%)[b]	Selectivity (7a:7b)[b]
1	$PhI(OAc)_2$	100	84:16
2[c]		85	95:5
3	PhIO	91	77:23
4	*m*-CPBA	100	40:60
5	TBHP	5	100:0
6	H_2O_2	3	100:0

[a] All reactions were performed with Mn^{III}(TPFC) (**6**) (1.0 µmol), OS (0.3 mmol), thioanisole (0.2 mmol), methanol (0.5 mL), water (5µL), reaction time (20 min), 25 °C. [b] Conversions and product selectivity were determined by GC-MS analysis with an internal standard (1,2,4-trichlorobenzene) in the crude reaction mixture. [c] Reaction with 1 equivalent of $PhI(OAc)_2$ (0.2 mmol).

3.2.4 Substrate scope

Further exploration into the substrate scope of the catalytic sulfoxidations by both manganese corrole and porphyrin catalysts were investigated under optimized conditions. The oxidized products and corresponding selectivities utilizing Mn^{III}(TPFPP)(ClO_3) (**2d**) and Mn^{III}(TPFC) (**6**) catalysts are listed in Table 4. In all cases, complete conversion of substituted thioanioles, high selectivity, and relatively short reaction times (<120 min) were achieved.

Various electron-donating or electron-withdrawing substituents in the aryl ring of thioanioles have a significant effect. As is evident in the results, the introduction of both electron-donating and electron-withdrawing groups resulted in reduced reactivity compared to thioanisole. In parallel to the porphyrin system, F^-, a substituent with stronger electron-withdrawing capabilities, gave higher reactivity than a Br^- substituent (**Table 4**, entries 2 and 3). A prolonged reaction time was required to achieve 100% conversion of the substrate with a methyl substituent as compared to a methoxy group (**Table 4**, entries 4 and 5). It is possible that the methoxy substituent is a stronger electron-donating group than the methyl substituent. Reduced reactivities were also observed in the corrole-manganese(III)-mediated sulfoxidation with *para*-substituted thioanisoles; a reaction time (20 min) was observed of the oxidations of *p*-fluorothioanisole and thioanisole (**Table 4**, entries 6 and 7). In the presence of chloro, bromo, and methyl substituted substrates, the reactions were slightly slower compared to thioanisole and the reactions resulted in complete conversion of sulfide within 30 min (**Table 4**, entries 8-10).

Table 4. Catalytic oxidation of substituted thioanisoles by manganese porphyrin (**2d**) and manganese corrole (**6**) with $PhI(OAc)_2$ [a]

Entry	Catalyst	Time (min)	Substrate	Product	Conversion (%)[b]	Yield (%)[b]
1	$Mn^{III}(TPFPP)(ClO_3)$ (**2d**)	30	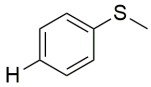	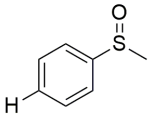	100	96
2		60	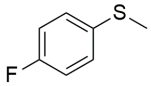	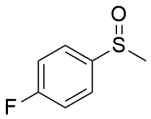	100	96
3		100	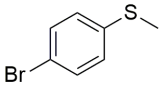	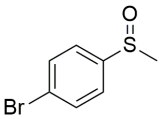	100	94
4		120	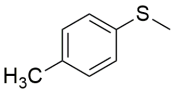	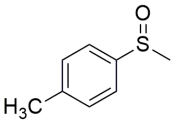	100	98
5		60	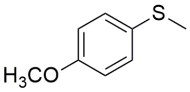	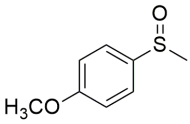	100	95
6	$Mn^{III}(TPFC)$ (**6**)	20	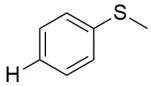	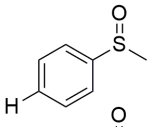	100	84
7		20	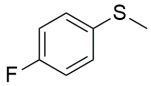	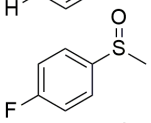	100	82
8		30	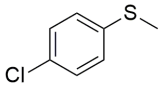	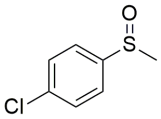	100	88
9		30	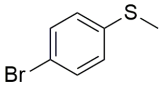	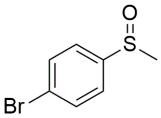	100	90
10		30	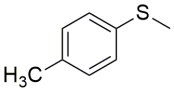	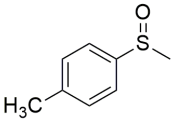	100	79

[a] All reactions were performed with $Mn^{III}(TPFPP)(ClO_3)$ (**2d**) and $Mn^{III}TPFC$ (**6**) (1.0 μmol), oxygen source (0.3 mmol), thioanisole (0.2 mmol), methanol (0.5 mL), water (5μL), , 25 °C. [b] Based on conversions of substrate and determined by quantitative GC-

MS analysis with an internal standard (1,2,4-trichlorobenzene) on the crude reaction mixture.

According to the kinetic study of (salen)manganese(III)-catalyzed oxidation of aryl phenyl sulfides by Chellamani et al., electron-donating substituents accelerate the reaction rate, while electron-withdrawing substituents slow down the rate.[34] However, the substituent effect was not observed for these reactions; both electron-donating and electron-withdrawing substituents moderately slow down the reactions, as seen in **Table 4**. It is noteworthy that monitoring catalytic reactions by UV-vis spectroscopy indicated no appreciable catalyst bleaching in the end of reactions. Control experiments demonstrated that no sulfoxide was formed in the absence of either the catalyst or $PhI(OAc)_2$.

4. PHOTOCHEMICAL GENERATION AND KINETIC STUDIES OF A PUTATIVE PORPHYRIN-RUTHENIUM(V)-OXO SPECIES

4.1 Introduction

In biomimetic catalytic oxidations, a transition metal catalyst is oxidized to a high-valent metal-oxo species by a sacrificial oxidant, and the activated transition metal-oxo intermediate then oxidizes the substrate.[12,51] However, high-valent metal-oxo species, such as metal(V)-oxo complexes, are extremely rare and difficult to detect because they are highly reactive. Detection and kinetic study of high-valent transition metal-oxo derivatives via a photochemical approach using laser flash photolysis (LFP) is of great interest because this method has greater access to the short-lived transients than the conventional rapid mixing methods. In this regard, we aim to explore the LFP photochemical approach targeting the direct detection and kinetic study of high-valent transition metal-oxo derivatives.

Among the high-valent metal-oxo species, porphyrin-ruthenium(V)-oxo transients have drawn much attention owing to their very efficient catalytic properties in oxidation reactions. In our previous studies, the ruthenium(IV)-μ-oxo bisporphyrins catalyzed efficient aerobic oxidation of alkenes and activated hydrocarbons using visible light and atmospheric oxygen.[52] In this section, we describe our findings on the photochemical formation of a highly reactive porphyrin-ruthenium(V)-oxo transient using LFP methods

and taking direct measurements of the rate constants for oxidation reactions. The same poprhyrin-ruthenium(V)-oxo species can also be produced using photo-induced ligand cleavage reactions achieved by its spectral and kinetic characteristics. Furthermore, the porphyrin-ruthenium(V)-oxo species showed excellent reactivity toward various organic substrates through kinetic studies.

4.2 Photo-disproportionation reaction

According to our previous studies, photolysis of a *bis*-corrole diiron(IV)-*μ*-oxo dimer proceeded via a disproportionation pathway that gave a corrole-iron(III) species and a corrole-iron(V)-oxo species.[53] Given the periodic relationship between ruthenium and iron and the nature of the similar macrocyclic system, it is possible that a ruthenium(V)-oxo intermediate and a ruthenium(III) porphyrin may be formed through a photo-disportionation reaction of a *bis*-porphyrin-diruthenium(IV)-μ-oxo dimer (**Scheme 14**). LFP method was employed to induce photolysis of the *bis*-porphyrin-diruthenium(IV)-μ-oxo dimer similar to those previously described for the diiron(IV)-*μ*-oxo-biscorrole complex.[53-54] Photolysis of the ruthenium dimer gave a transient species that decayed on a 50 ms scale followed by a slow growth on an 1 s scale (**Figure 19A**). The time-resolved *difference* spectrum (**Figure 19B**) is defined as spectrum (t) – spectrum (final) as is conventional in LFP studies. In this representation, positive absorbances are from the species decaying with time, whereas growing peaks have negative absorbances from the species forming with time. Irradiation of the complex $[Ru^{IV}(TPP)(OH)]_2O$ (**4**) with 355 nm laser light at ambient temperature in CH_3CN

solution generated a homolytic cleavage through the Ru-O bond which instantly produced a highly reactive transient (**10**) displaying a strong Soret band at 390 nm, which rapidly decayed to form [Ru^{III}(TPP)(OH)] (**11**) with Soret band at 410 nm and Q band at 530 nm (**Figure 19B**). The spectrum of the photo-product (**11**) was identical to that of Ru^{III}(TPP)(OH), which was independently prepared from the reported method.[55] In a slower subsequent phase of the reaction (**Figure 19C**), we believe that exposing the photo-product of **11** to oxygen led to regeneration of the diruthenium(IV)- μ-oxo complex through an auto-oxidation pathway.[56]

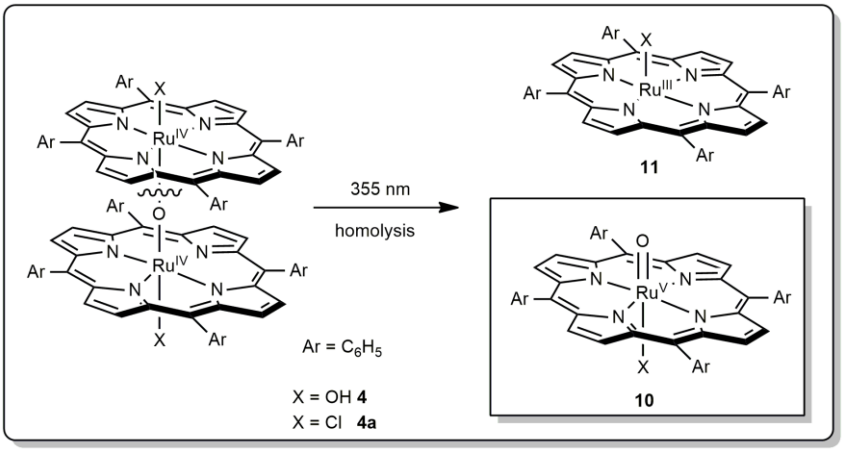

Scheme 14. Photo-disproportionation approach to form the putative porphyrin-ruthenium(V)-oxo species.

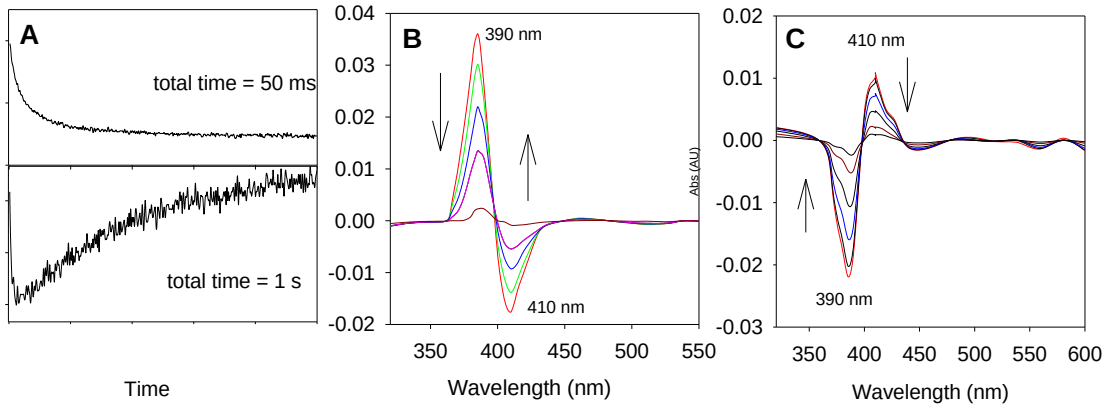

Figure 19. (A) Kinetic trace at λ_{max} (390 nm) showing a rapid decay over 50 ms followed by a slow growing process over 1 s after laser pulse; (B) Time-resolved difference spectra following 355 nm irradiation of **4** in the presence of benzophenone (10 mM) in CH_3CN at 22 ^{o}C. (C) Time-resolved difference spectra over 1 s following 355 nm irradiation of **11** in the presence of benzophenone (10 mM) in oxygen-saturated CH_3CN. In this period, the species **11** is converting to μ-oxo ruthenium(IV) dimer.

In this investigation, we have also discovered that the choice of axial ligand on the metal of the dimer gave different effects. The activity of the dimer with a chloride axial (**4a**) ligand was significantly lower than that of a dimer with a hydroxyl ligand (**4**). In LFP reactions when a dimer with a chloride ligand (**4a**) was employed under identical conditions as those described for **4**, there was no evidence of a transient species at 390 nm or 410 nm being formed; instead, only a rapid reformation process of the starting precursor (**4a**) was observed (**Figure 20**). The LFP results suggest that the photolysis of **4a** mainly occurs at the Ru-Cl bond which gave ruthenium(IV) and chlorine radical followed by a rapid recombination reaction.

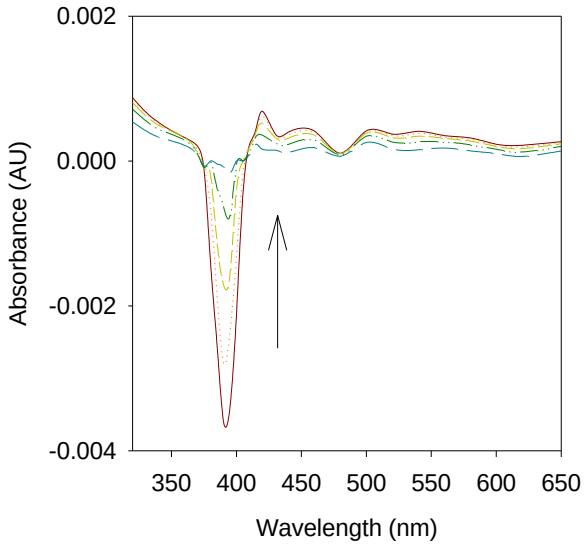

Figure 20. Time-resolved difference spectrum following 355 nm irradiation of $[Ru^{IV}(TPP)Cl]_2O$ (**4a**) in the presence of benzophenone (10 mM) in CH_3CN at 22 ^oC; difference spectrum =spectrum(t) - spectrum (final= 20 ms).

4.3 Photo-induced ligand cleavage reaction

In addition, we have discovered an alternate route to produce the same ruthenium(V)-oxo species through a photosynthetic pathway. In our previous work, we reported a new photosynthetic entry to the well-known *trans*-dioxo-ruthenium(VI) porphyrins as a result of the simultaneous cleavage of the two X-O bonds from ruthenium(IV) dichlorates or dibromates.[52, 57] In this work, we have also extended the so called photo-induced cleavage reaction[54] for the generation of ruthenium(V)-oxo species. Instead of the homolysis of the Cl-O in ruthenium(IV) dichlorates that gave an one-electron oxidation, we expected a two-electron oxidation through heterolysis of the O-X bond in the oxygen-containing ligands to produce the ruthenium(V)-oxo species (**Scheme 15**).

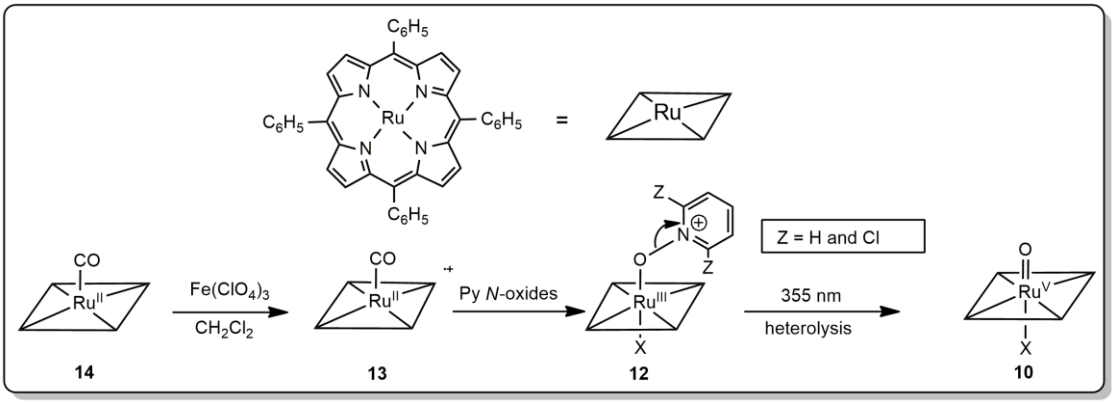

Scheme 15. Generation of the porphyrin-ruthenium(V)-oxo species (**10**) via a photo-induced ligand cleavage reaction.

Based on Groves and coworkers' early study, it is generally accepted that the pyridine *N*-oxide/Ru^{III} complex is the precursor in the catalytic cycle that eliminates pyridine on heterolytic fragmentation to form the ruthenium(V)-oxo species as the active oxidant.[19, 55] Following the literature reported procedure, the ruthenium(II) porphyrin radical cation (**13**) (**Figure 21**, dashed line) was generated by the oxidation the carbonyl precursor (**14**) (**Figure 21**, dotted line) with ferric perchlorate with in CH_2Cl_2 at room temperature. Addition of excess pyridine *N*-oxide or 2,6-dicholoropyridine *N*-oxide led to the formation of a ruthenium(III) *N*-oxide adduct (**12**) which showed a distinct UV-vis absorption that consistent with the reported value (**Figure 21**, solid line).[55] As expected, species (**13**) shows the EPR signal (g = 2.000) in agreement with the proposed structure (**Figure 21**, inset).

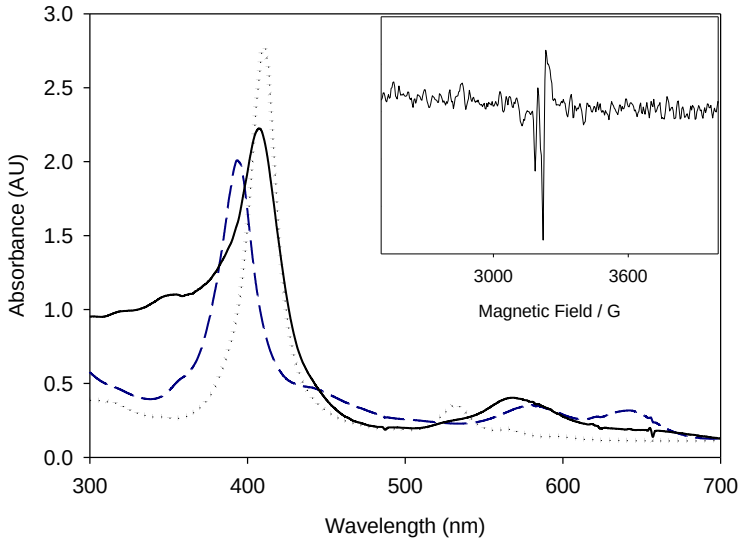

Figure 21. Superimposed UV-visible spectra of ruthenium(III) *N*-oxide adduct (**12**) (solid lines), ruthenium (II) porphyrin radical cation (**13**) (dashed line) and carbonyl precursor (**14**) (dotted lines) at room temperature in CH_2Cl_2. Inset: X-band EPR of **13** at 298 K.

By subjecting the complex to a 355 nm laser light, we observed the creation of a highly reactive ruthenium(V) transient which was monitored by UV-visible spectroscopy. In a time-resolved difference spectrum (**Figure 22A**), this ruthenium transient was characterized by a Soret band absorbance at λ_{max} 390 nm. The formed intermediate decayed to a ruthenium(III) species with an absorbance of 410 nm with a 45 ms half-life in the absence of organic reductants in CH_2Cl_2 (**Figure 22A**). When organic substrate such as cyclohexene was present, the decay of the photochemically-generated species accelerated linearly with the substrate concentration (**Figure 22B**), indicating a second-order reaction. From the linear plot, the second-order rate constant of 740 M^{-1} s^{-1} was calculated. According to the spectral and kinetic behavior, we further confirmed that the transient generated by this path was identical to the intermediate formed by the photo-disproportionation reaction.

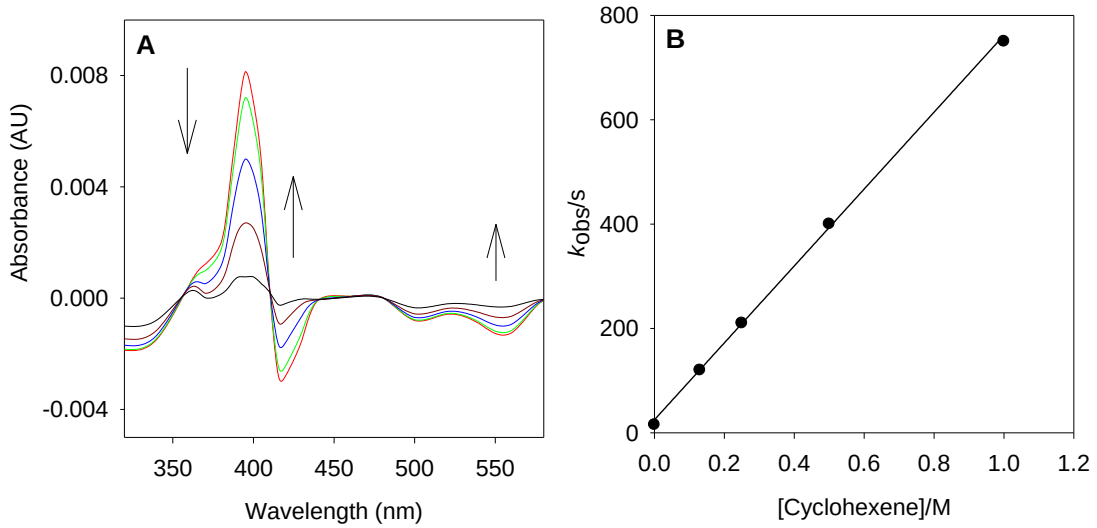

Figure 22. (A) Time-resolved difference spectrum following 355 nm irradiation of meta-stable intermediate (**12**) over 100 ms in CH_2Cl_2 at 22 ^oC. (B) Observed rate constants for reactions with cyclohexene in CH_2Cl_2 at 22 ^oC, monitored at 390 nm.

4.4 Kinetic studies

Kinetic studies were accomplished by generating ruthenium(V)-oxo species (**10**) using photo-disproportionation reactions in the presence of organic substrates at varying high concentrations under pseudo-first-order conditions. In all kinetic measurements, we monitored decay of the Soret band for the ruthenium(V)-oxo species at 390 nm. The background rate constant (k_0) was formulated by the pseudo first order decay rate constant of the absence of the substrate when the species (**10**) reacted rapidly in CH_3CN solution. Presumably, the background reaction is due to reaction of **10** with the solvent or organic impurities. In the presence of organic substrates, the pseudo-first-order decay rate constants increased linearly with substrate concentration. The kinetics are described by

Eq. 1, where k_{obs} is the observed pseudo first order rate constant and k_{ox} was the second order rate constant which is affected by the substrate concentration [substrate].

$$k_{obs} = k_0 + k_{ox}[\text{substrate}] \qquad \text{(Eq. 1)}$$

The kinetic plots from reactions of **10** formed by photolysis of **4** with representative organic substrates are shown graphically in **Figure 23**, where plots of k_{obs} versus the concentrations of different substrates were linear, and the second-order rate constants for reactions of **10** with other substrates are collected in **Table 5**.

Organic substrates such as alkenes and benzylic alcohols with the reactions of species **10** were investigated in the kinetic study. The rate constants listed in Table 5 demonstrate that oxidation of benzylic alcohols is faster than oxidation of alkenes, possibly owing to a more energetically favorable mechanism. We noticed by the addition of small amount of CH_3OH (5% v/v) that the reaction of cyclohexene with ruthenium(V)-oxo transient slowed down compared to the reaction under identical conditions in the absence of CH_3OH (Table 1, entry 2 and 3). In contrast, the reaction was three times faster when performed in CH_3CN ($k_{ox} = 1.8 \times 10^3$, entry 2, **Table 5**) compared to CH_2Cl_2 ($k_{ox} = 7.4 \times 10^2$, entry 4, **Table 5**). This phenomena can be explained by the ligation of the solvent to the ruthenium(V) center thus affecting the transients' reactivity toward oxidation of cyclohexene.

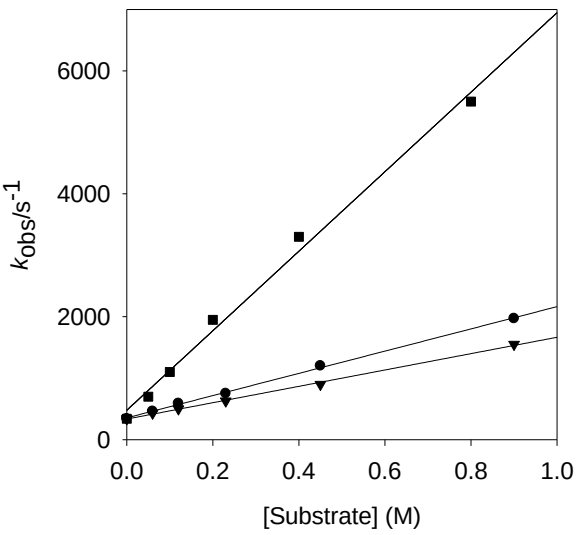

Figure 23. Representative plots of observed pseudo-first-order rate constants for reaction of species **10** versus concentrations of diphenylmethanol (square), cyclohexene (circles) and *cis*-cyclooctene (triangles) in CH_3CN.

Table 5. Second-order rate constants for reactions of porphyrin-ruthenium(V)-oxo intermediate [a].

Entry	Substrate	k_{ox} (M^{-1} s^{-1})
1	none[b]	340 s^{-1}
2	cycloohexene	$(1.8 \pm 0.2) \times 10^3$
3[c]		$(1.2 \pm 0.2) \times 10^3$
4[d]		$(7.4 \pm 0.6) \times 10^2$
5	*cis*-cyclooctene	$(1.3 \pm 0.3) \times 10^3$
6	styrene	$(2.5 \pm 0.3) \times 10^3$
7	α-methylstyrene	$(1.8 \pm 0.1) \times 10^3$
8	diphenylmethanol	$(6.6 \pm 0.6) \times 10^3$
9	1-phenylethanol	$(8.6 \pm 0.7) \times 10^3$

[a] Reactions at 22 ± 2 °C under single-turnover conditions in CH_3CN except otherwise specified. Standard deviations are 2σ. [b] Pseudo-first-order decay rate constant in the absence of substrate, defined as background rate constant (k_0). [c] CH_3CN:CH_3OH (v/v = 20:1). [d] in CH_2Cl_2

The k_{ox} values determined in this work provide a quantitative comparison of the kinetics of reactions of the porphyrin-ruthenium(V)-oxo species (**10**) to those of related porphyrin/corrole-metal-oxo complexes. In the alkene epoxidations by the well-characterized *trans*-dioxoruthenium(VI) porphyrins, the second order rate constants obtained under similar conditions are in the ranges of 4.0×10^{-3} to 4.1×10^{-2} M^{-1} s^{-1}.[58] Remarkably, the observed rate constants for reactions of **10** with cyclohexene and other organic substrates (**Table 5**) are 5-6 orders of magnitude greater than those for similar reactions of the *trans*-dioxoruthenium(VI) complexes including much more electron-demanding porphyrin system.[58]

5. CONCLUSION

Manganese(III) porphyrins and manganese(III) corroles catalyze the highly efficient oxidation of sulfides to sulfoxides with $PhI(OAc)_2$ in presence of small amount of water. Various thioanisoles could be successfully oxidized with complete conversion of sulfide and excellent selectivity. The effect of axial ligand on the reactivity of Mn^{III}(TPFPP)X in oxidation reactions was observed and the weakly binding perchlorate gave the highest catalytic activity in the oxidation of sulfide. The remarkably enhanced catalytic activity and stability against degradation is ascribed to the slow and steady-state formation of PhIO from well soluble $PhI(OAc)_2$ in presence of small amount of water. Although metalloporphyrin catalysts exhibit lower reactivity compared to metallocorrole catalysts under identical conditions, no bleaching of the metalloporphyrin catalysts in the end of the oxidation reactions was obtained. Thus, metalloporphyrin catalysts show a better stability compared to metallocorroles in sulfide oxidations.

We have demonstrated the generation of the ruthenium(V)-oxo and a ruthenium(III) porphyrin species that occurred in a homolytic cleavage through a photo-disportionation reaction of a *bis*-porphyrin-ruthenium(IV) μ-oxo dimer. Laser flash photolysis production of poprhyrin-ruthenium(V)-oxo species has permitted the detection of the highly reactive intermediates in organic solvents and direct kinetic studies of their reactions with typical organic substrates. More importantly, the photo-cleavage of a ruthenium(III) *N*-oxide adduct proceeds by heterolysis of Ru-O bond to give an oxo transient that is

spectroscopically and kinetically indistinguishable from the species formed by photolysis of the corresponding bisporphyrin-ruthenium(IV) μ-oxo dimer, confirming that the same oxidizing ruthenium(V)-oxo species was produced from both methods. Second-order rate constants for reactions with several substrates were obtained. Further studies to characterize the observed transients more fully and to define synthetic applications are ongoing in our laboratory.

REFERENCES

1. Baeckvall, J. E., *Modern oxidation methods*. Wiley-VCH Verlag: Weinheim, 2004.

2. Shilov, A. E.; Shulpin, G. B., Activation of C-H bonds by metal complexes. *Chem. Rev.* **1997,** *97*, 2879-2932.

3. Jiang, G. F.; Liu, Q.; Guo, C. C., Biomimetic Oxidation of Hydrocarbons with Air over Metalloporphyrins. In *Biomimetic Based Applications*, George, A., Ed. InTech: 2011.

4. McGown, A. J.; Badiei, Y. M.; Leeladee, P.; Prokop, K. A.; Debeer, S.; Goldberg, D. P., Synthesis and Reactivity of High-Valent Transition Metal Corroles and Corrolazines. In *Handbook of Porphyrin Science*, Kadish, K. M., Smith, K. M., Guilard, R., Ed. World Scientific Press: 2011.

5. Zhang, R.; Vanover, E.; Chen, T.-H.; Thompson, H., Visible light-driven aerobic oxidation catalyzed by a diiron(IV) μ-oxo biscorrole complex. *Appl. Catal. A* **2013,** *465*, 95-100.

6. Zhang, R., Asymmetric Organic Oxidation by Chiral Ruthenium Complexes Containing D_2- and D_4- Symmetric Porphyrinato Ligands. *Ph. D. Thesis* **2000**, 1-235.

7. Sono, M.; Roach, M. P.; Coulter, E. D.; Dawson, J. H., Heme-Containing Oxygenases. *Chem. Rev.* **1996,** *96*, 2841-2887.

8. Newcomb, M.; Zhang, R.; Chandrasena, R. E. P.; Halgrimson, J. A.; Horner, J. H.; Makris, T. M.; Sligar, S. G., Cytochrome P 450 compound I. *J. Am. Chem. Soc.* **2006,** *128*, 4580-4581.

9. Vatsis, P. K.; Peng, -. M. H.; Coon, J. M., Replacement of active-site cysteine-436 by serine converts cytochrome P450 2B4 into an NADPH oxidase with negligible monooxygenase activity. *J. Inorg. Biochem.* **2002,** *91*, 542-553.

10. Aldag, C.; Gromov, I.; García-Rubio, I.; Koenig, v. K.; Schlichting, I.; Jaun, B.; D., H., Probing the role of the proximal heme ligand in cytochrome P450cam by recombinant incorporation of selenocysteine. *Proc Natl Acad Sci U S A.* **2009,** *106*, 5481-5486.

11. Yoshioka, S.; Takahashi, S.; Hori, H.; Ishimori, K.; Morishima, I., Proximal cysteine residue is essential for the enzymatic activities of cytochrome P450cam. *Eur J Biochem* **2001,** *268* (252-9).

12. Meunier, B., *Metal-Oxo and Metal-Peroxo Species in Catalytic Oxidations*. Springer-Verlag: Berlin, 2000.

13. Denisov, I. G.; Makris, T. M.; Sligar, S. G.; Schlichting, I., Structure and chemistry of cytochrome P 450. *Chem. Rev.* **2005,** *105*, 2253-2277.

14. Zhang, R.; Nagraj, N.; Lansakara-P, D. S. P.; Hager, L. P.; Newcomb, M., Kinetics of Two-Electron Oxidations by the Compound I Derivative of Chloroperoxidase, a Model for Cytochrome P450 Oxidants. *Org. Lett.* **2006,** *8*, 2731-2734.

15. Groves, J. T.; Nemo, T. E.; Myers, R. S., Hydroxylation and epoxidation catalyzed by iron-porphine complexes. Oxygen transfer from iodosylbenzene. *J. Am. Chem. Soc.* **1979,** *101*, 1032-1033.

16. Groves, J. T., Shalyaev, K.; Lee, J., Oxometalloporphyrins in Oxidative Catalysis. In *The Porhyrin Handbook*, Kadish, K. M. S., K. M.; Guilard, R., Ed. 2000; Vol. 4, pp 17-40.

17. Nam, W., High-Valent Iron(IV)–Oxo Complexes of Heme and Non-Heme Ligands in Oxygenation Reactions. *Acc. Chem. Res.* **2007,** *40*, 522-531.

18. Groves, J. T.; Lee, J.; Marla, S. S., Detection and Characterization of an Oxomanganese(V) Porphyrin Complex by Rapid-Mixing Stopped-Flow Spectrophotometry. *J. Am. Chem. Soc.* **1997,** *119*, 6269-6273.

19. Wang, C.; Shalyaev, K. V.; Bonchio, M.; Carofiglio, T.; Groves, J. T., Fast Catalytic Hydroxylation of Hydrocarbons with Ruthenium Porphyrins. *Inorg. Chem.* **2006,** *45*, 4769-4782.

20. Gross, Z.; Gray, H. B., Oxidations catalyzed by metallocorroles. *Adv. Syn. Catal.* **2004,** *346*, 165-170.

21. Visser, S. P. d.; Ogliaro, F.; Gross, Z.; Shaik, S., What Is the Difference between the Manganese Porphyrin and Corrole Analogues of Cytochrome P450's Compound I? *Chem. Eur. J.* **2001,** *7*, 4954-4960.

22. Grigg, R.; Hamilton, R. J.; Jozefowicz, M. L.; Rochester, C. H.; Terrell, R. J.; Wickwar, H., A Spectroscopic Study of the Protonation of Porphins and Corroles. *J. Chem. Soc., Perkin Trans.* **1973**, 407-413.

23. Gross, Z.; Galili, N.; Simkhovich, L.; Saltsman, I.; Botoshansky, M.; Blaeser, D.; Boese, R.; Goldberg, I., Solvent-Free Condensation of Pyrrole and Pentafluorobenzaldehyde: A Novel Synthetic Pathway to Corrole and Oligopyrromethenes. *Org. Lett.* **1999,** *1*, 599-602.

24. Johnson, A. W.; Kay, I. T., 306. Corroles. Part I. Synthesis. *J. Chem. Soc., Perkin Trans.* **1965**, 1620-1629.

25. Gross, Z.; Simkhovich, L.; Galili, N., First catalysis by corrole metal complexes: epoxidation, hydroxylation, and cyclopropanation. *Chem. Commun.* **1999**, 599-600.

26. Mahammed, A.; Gross, Z., Albumin-Conjugated Corrole Metal Complexes: Extremely Simple Yet Very Efficient Biomimetic Oxidation Systems. *J. Am. Chem. Soc.* **2005,** *127*, 2883-2887.

27. Mahammed, A.; Gray, H. B.; Meier-Callahan, A. E.; Gross, Z., Aerobic Oxidations Catalyzed by Chromium Corroles. *J. Am. Chem. Soc.* **2003,** *125*, 1162-1163.

28. Cho, K.; Leeladee, P.; McGown, A. J.; DeBeer, S.; Goldberg, D. P., A High-Valent Iron−Oxo Corrolazine Activates C−H Bonds via Hydrogen-Atom Transfer. *J. Am. Chem. Soc.* **2012,** *134*, 7392-7399.

29. Kowalski, P.; Mitka, K.; Ossowska, K.; Kolarska, Z., Oxidation of sulfides to sulfoxides. Part1: Oxidation using halogens derivatives. *Tetrahedron* **2005,** *61*, 1933-1953.

30. Nehlsen, J. P.; Benziger, J. B.; Kevrekidis, I. G., Removal of alkanethiols from a hydrocarbon mixture by a heterogeneous reaction with metal oxides. *Ind. Eng. Chem. Res.* **2003,** *42*, 6919-6923.

31. Caron, S.; Dugger, R. W.; Ruggeri, S. G.; Ragan, J. A.; Ripin, D. H. B., Large-Scale Oxidations in the Pharmaceutical Industry. *Chem. Rev.* **2006,** *106*, 2943-2989.

32. Wojaczynska, E.; Wojacznski, J., Enantioselective Synthesis of Sulfoxides: 2000-2009. *Chem. Rev.* **2010,** *110*, 4303-4356.

33. Hosseinpoor, F.; Golchoubian, H., Mn(III)-Catalyzed Oxidation of Sulfides to Sulfoxides with Hydrogen Peroxide. *Tetrahedron Lett.* **2006,** *47*, 5195-5197.

34. Chellamani, A.; Alhaji, N. I.; Rajagopal, S., Kinetics and Mechanism of (salen)Mn^{III}-Catalysed Hydrogen Peroxide Oxidation of Alkyl Aryl Sulphides. *J. Phys. Org. Chem.* **2007,** *20*, 255-263.

35. Watanabe, Y.; Fujii, H., Characterization of High-Valent Oxo-Metalloporphyrins. In *Metal-Oxo and Metal-Peroxo Species in Catalytic Oxidations*, Meunier, B., Ed. Springer-Verlag: Berlin, 2000.

36. Davies, J., Selective hydrocarbon activation: Principle and progress. VCH: New York: 1994.

37. Lindsey, J.; Wagner, R. D., Investigation of the synthesis of ortho-substituted tetraphenylporphyrins. *J. Org. Chem.* **1989,** *54*, 828-836.

38. Adler, A. D.; Longo, F. R.; Finarelli, J. D.; Goldmacher, J.; Assour, J.; Korsakoff, L., A Simplified synthesis for *meso*-Tetraphenylporphin. *J. Org. Chem.* **1966,** *32*, 476.

39. Che, C.-M.; Huang, J.-S., Metalloporphyrin-based oxidation systems: from bioimetic reactions to application in organic synthesis. *Chem. Commun.* **2009**, 3996-4015.

40. Lo, W.-C.; Che, C.-M.; Cheng, K.-F.; Mak, T. C. W., Catalytic and asymmetric cyclopropanation of styrenes catalysed byruthenium porphyrin and porphycene complexes. *Chem. Commun.* **1997**, 1205-1206.

41. Sugimoto, H.; Higashi, T.; Mori, M.; Nagano, M.; Yoshida, Z.; Ogoshi, H., Preparation and physicochemical properties of new linear m-oxo bridged ruthenium(IV) and osmium(IV) porphyrin dimers. *Bull. Chem. Soc.Jpn.* **1982,** *55*, 822-8.

42. Kumar, A.; Botoshansky, M.; Buchman, Y.; Gross, Z., Oxygen Atom Transfer Reactions from Isolated (Oxo)manganese(V) Corroles to Sulfides. *J. Am. Chem. Soc.* **2010,** *132*, 15233-15245.

43. Kwong, K. W.; Chen, T. H.; Luo, W.; Jeddi, H.; Zhang, R., A biomimetic oxidation catalyzed by manganese(III) porphyrins and iodobenzene diacetate: Synthetic and mechanistic investigations. *Inorg. Chim. Acta* **2015,** *430*, 176-183.

44. Aviv, I.; Gross, Z., Corrole-based applications. *Chem. Commun.* **2007,** *20*, 1987-1999.

45. Goldberg, D. P., Corrolazines: New Frontiers in High-Valent Metalloporphyrinoid Stability and Reactivity. *Acc. Chem. Res.* **2007,** *40*, 626-634.

46. Chen, T.-H.; Kwong, K.-W.; Carver, A.; Luo, W. L.; Zhang, R., Enhanced iron(III) corrole-catalyzed oxidations with iodobenzene diacetate: Synthetic and mechanistic investigations. *Appl. Catal. A* **2015,** *497*, 121-126.

47. Gross, Z.; Nimri, S., A Pronounced Axial Ligand Effect on the Reactivity of Oxoiron(IV) Porphyrin Cation Radicals. *Inorg. Chem.* **1994,** *33*, 1731-1732.

48. Urano, Y. H., T.; Hirobe, M.; Nagano, T., Pronounced Axial Thiolate Ligand Effect on the Reactivity of High-Valent Oxo-Iron Porphyrin Intermediate. *J. Am. Chem. Soc.* **1997,** *119*, 12008-12009.

49. Liao, M.-S.; Huang, M.-J.; Watts, J. D., Iron Porphyrins with Different Imidazole Ligands. A Theoretical Comparative Study. *J. Phys. Chem. A* **2010,** *114*, 9554-9569.

50. Nam, W.; Kim, I.; Lim, M. H.; Choi, H. J.; Lee, J. S.; Jang, H. G., Isolation of an oxomanganese(V) porphyrin intermediate in the reaction of a manganese(III) porphyrin complex and H2O2 in aqueous solution. *Chem. Eur. J.* **2002,** *8*, 2067-2071.

51. Costas, M.; Mehn, M. P.; Jensen, M. P.; Que, L., Dioxygen Activation at Mononuclear Nonheme Iron Active Sites: Enzymes, Models, and Intermediates. *Chem. Rev.* **2004,** *104*, 939-986.

52. Vanover, E.; Huang, Y.; Xu, L.; Newcomb, M.; Zhang, R., Photocatalytic Aerobic Oxidation by a bis-Porphyrin-Ruthenium(VI) μ-Oxo Dimer: Observation of a Putative Porphyrin-Ruthenium(V)-Oxo Intermediate. *Org. Lett.* **2010,** *12*, 2246-2249.

53. Harischandra, D. N.; Lowery, G.; Zhang, R.; Newcomb, M., Production of a Putative Iron(V)−Oxo Corrole Species by Photo-Disproportionation of a Bis-Corrole−Diiron(IV)−μ-Oxo Dimer: Implication for a Green Oxidation Catalyst. *Org. Lett.* **2009,** *11*, 2089-2092.

54. Zhang, R.; Newcomb, M., Laser Flash Photolysis Generation of High-Valent Transition Metal-Oxo Species: Insights from Kinetic Studies in Real Time. *Acc.Chem. Res.* **2008,** *41*, 468-477.

55. Groves, J. T.; Bonchio, M.; Carofiglio, T.; Shalyaev, K., Rapid Catalytic Oxygenation of Hydrocarbons by Ruthenium Pentafluorophenylporphyrin Complexes: Evidence for the Involvement of a Ru(III) Intermediate. *J. Am. Chem. Soc.* **1996,** *118*, 8961-8962.

56. Collman, J. P.; Barnes, C. E.; Brothers, P. J.; Collins, T. J.; Ozawa, T.; Gallucci, J. C.; Ibers, J. A., Oxidation of ruthenium(II) and ruthenium(III) porphyrins. Crystal structures of m-oxo-bis[(p-methylphenoxo)(meso-tetraphenylporphyrinato)ruthenium(IV)] and ethoxo(meso-tetraphenylporphyrinato)(ethanol)ruthenium(III)-bisethanol. *J. Am. Chem. Soc.* **1984,** *106*, 5151-63.

57. Zhang, R.; Huang, Y.; Abebrese, C.; Thompson, H.; Vanover, E.; Webb, C., Generation of trans-dioxoruthenium(VI) porphyrins: A photochemical approach. *Inorg. Chim. Acta* **2011,** *372*, 152-157.

58. Che, C.-M.; Zhang, J.-L.; Zhang, R.; Huang, J.-S.; Lai, T.-S.; Tsui, W.-M.; Zhou, X.-G.; Zhou, Z.-Y.; Zhu, N.; Chang, C. K., Hydrocarbon oxidation by beta-Halogenated dioxoruthenium(VI) porphyrin complexes: Effect of reduction potential (RuVI/V) and C-H bond-dissociation energy on rate constants. *Chem. Eur. J* **2005,** *11*, 7040-7053.

CURRICULUM VITAE

Articles in peer-reviewed journals

- Kwong, K.W.; Chen, T.-H.; Luo, W. L.; Jeddi, H.; Zhang, R., A biomimetic oxidation catalyzed by manganese(III) porphyrins and iodobenzene diacetate: Synthetic and mechanistic investigations. *Inorg. Chim. Acta* **2015,** *430*, 176-183
- Chen, T.-H.; Kwong, K.W.; Carver, A.; Luo, W. L.; Zhang, R., Enhanced iron(III) corrole-catalyzed oxidation with iodobenzene diacetate: Synthetic and Mechanistic Implications. *Appl. Catal. A* **2015**, *497*, 121-126.
- Zhang, R.; Vanover. E; Luo, W. L.; Newcomb, M., Photochemical generation and kinetic studies of a putative porphyrin-ruthenium(v)-oxo species. *Dalton Trans*, **2014**, *43*, 8749

Presentations at academic conferences

National

- Luo, W.L.; Chen, T.-H.; Yuan, Z.; Zhang, R. "Visible light-promoted selective sulfoxidations catalyzed by ruthenium porphyrins with iodobenzene diacetate." 249th American Chemistry Society National Meeting & Exposition, Denver, CO, March 2015
- Luo, W.L.; Vanover, E.; Zhang, R. "Photochemical generation and kinetic studies of a putative porphyrin-ruthenium(v)-oxo species." 248th American Chemistry Society National Meeting & Exposition, San Francisco, CA, August 2014.

Regional

- Luo, W.L.; Zhang, R. "Solvent effect on selective sulfoxidation catalyzed by manganese(III) corrole complexes." 101th Kentucky Academy of Science Annual Meeting, Highland , KY, November 2015.
- Luo, W.L.; Vanover, E.; Zhang, R. "An efficient photocatalytic oxidation through a highly reactive porphyrin-euthenium(V)-oxo species." 100th Kentucky Academy of Science Annual Meeting, Lexington, KY, November 2014.
- Luo, W.L.; Vanover, E.; Zhang, R. "Photochemical generation and kinetic study of a highly reactive porphyrin-ruthenium(V)-oxo species for Photocatalytic Aerobic Oxidations." Southeastern Regional Meeting of American Chemistry Society, Nashville, TN, October 2014.
- Luo, W.L.; Chen, T.-H.; Zhang, R. "Selective oxidation of sulfides to sulfoxides catalyzed by manganese (III) porphyrin complexes with different axial ligands." 99th Kentucky Academy of Science Annual Meeting, Morehead, KY, November 2013.

Local

- Luo, W.L.; Zhang, R. "Synthetic and catalytic oxidation studies by metalloporphyrins and metallocorroles." WKU Student Research Conference, Bowling Green, KY, March 2016
- Luo, W.L.; Zhang, R. "Selective sulfoxidation catalyzed by manganese(III) porphyrin complexes with different axial ligands." WKU Student Research Conference, Bowling Green, KY, March 2015

- Luo, W.L.; Chen, T.-H.; Zhang, R. “Axial ligand effect on catalytic oxidation of sulfides by manganese (III) porphyrin complexes.” WKU Student Research Conference, Bowling Green, KY, March 2014.